

AD-A171 613

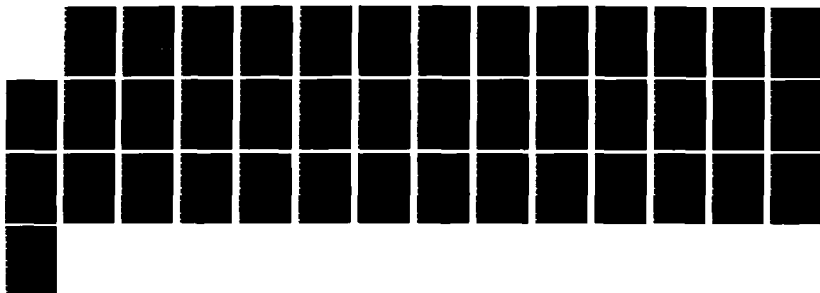
SHAPE FROM TEXTURE: GENERAL PRINCIPLE(U) MARYLAND UNIV  
COLLEGE PARK CENTER FOR AUTOMATION RESEARCH  
K KANATANI ET AL FEB 86 CAR-TR-184 DAAK78-83-K-0018

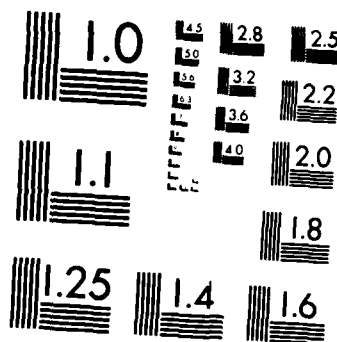
1/1

UNCLASSIFIED

F/G 6/4

NL





MICROCOPY RESOLUTION TEST CHART  
NATIONAL BUREAU OF STANDARDS-1963-A

AD-A171 613

CAR-TR-184  
CS-TR-1618

• DAAK70-83-K-0018  
February 1986

SHAPE FROM TEXTURE: GENERAL PRINCIPLE

Ken-ichi Kanatani\*  
Tsai-Chia Chou  
Center for Automation Research  
University of Maryland  
College Park, MD 20742

DTIC  
ELECTE

SEP 5 1986

COMPUTER VISION LABORATORY

CENTER FOR AUTOMATION RESEARCH

This document has been approved  
for public release and sale; its  
distribution is unlimited.

UNIVERSITY OF MARYLAND  
COLLEGE PARK, MARYLAND  
20742

86 9 5 054

2

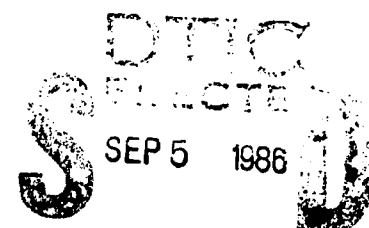
CAR-TR-184  
CS-TR-1618

DAAK70-83-K-0018  
February 1986

# SHAPE FROM TEXTURE: GENERAL PRINCIPLE

Ken-ichi Kanatani\*  
Tsai-Chia Chou

Center for Automation Research  
University of Maryland  
College Park, MD 20742



## ABSTRACT

The 3D shape of a textured surface is recovered from its projected image on the assumption that the texture is homogeneously distributed. First, the homogeneity of a discrete texture consisting of dots and line segments is defined in terms of the theory of distributions. Next, distortion of the observed texture density due to perspective projection is described in terms of the first fundamental form, which is expressed with respect to the image coordinate system. Based on this result, the basic equations to determine the surface shape are derived for both planar and curved surfaces, and numerical schemes are proposed to solve them. Necessary data are obtained in the form of summation or integration of functions over the texture elements on the image plane. Ambiguity in the interpretation of curved surfaces is also analyzed. Finally, numerical examples for synthetic data are presented, and our method is compared with other existing methods. It is shown that all other methods can be explained in terms of our formulation.

This document is hereby released for public release and distribution.

The support of the Defense Advanced Research Projects Agency and the U.S Army Night Vision and Electro-Optics Laboratory under Contract DAAK70-83-K-0018 is gratefully acknowledged.

\*Permanent Address: Department of Computer Science, Gunma University, Kiryu, Gunma 376, Japan

86-9-5-054

## 1. INTRODUCTION

The recovery of the 3D shape of a surface from its projected image is one of the most important challenges in computer vision. The computation is based on various clues such as texture, shading and motion. 3D recovery from texture is possible if we have some knowledge about the *true* texture. If the projected texture has different properties from those of the true texture, the 3D shape is recovered from the difference between the observed properties and the original properties that we know. For example, if the true texture is known to be an array of texture elements of a known shape, the surface shape can be inferred from the observed distortion of the texture elements.

If we do not know the true texture but know its *statistical* properties, we can draw an inference from the difference between the observed statistical properties and the true properties. Assumptions often adopted are *homogeneity* and *isotropy* of the true texture. The assumption of isotropy asserts that the texture consists of line segments with no preferred orientations. A clue for 3D recovery is obtained if the observed texture segments have a preferred orientation. This approach was first investigated by Witkin [1], and the algorithm was improved by Davis, et al. [2]. Kanatani [3] gave a rigorous mathematical description of the problem and explicit formulae to solve the problem by means of tensor calculus and the principle of *stereology*.

The assumption of homogeneity, on the other hand, asserts that the texture is uniformly distributed over the surface. When projected, the texture becomes dense on the image of the surface part away from the observer and sparse on the part near the observer. This clue has been considered long since by people like Gibson [4, 5], Bajcsy and Lieberman [6] and Stevens [7], but their argument was based on naive intuition. It was not until Aloimonos and Swain [8] and Dunn [9] that the problem was treated in analytical terms based on the geometry of perspective projection. However, their formulations involve many unnecessary *ad hoc* approximations and assumptions. In this paper, we show a mathematically rigorous treatment based on *differential geometry* and the *theory of distributions*, taking the "discreteness" of texture correctly into account.

We first give a precise definition of *homogeneity* of a texture. If a texture consists of dots or line segments, the *texture density* is a singular function taking the value infinity at the texture dots and line segments and 0 elsewhere. How can we say that the density is uniform? How can we tell that a given texture is homogeneous? We will give an exact definition of homogeneity of a discrete texture.

We next give an exact analysis of the distortion of texture due to perspective projection in terms of the *first fundamental form* expressed with respect to the image coordinate system. Our formulation consists of two stages. First, we present the basic equations to determine the surface shape for both planar and curved surfaces in their *exact* forms. Although they are difficult to solve directly, we can infer various theoretical consequences, among which is the ambiguity in the interpretation of curved surfaces. We list all possibilities completely.

Then, we propose various numerical schemes to solve these equations, employing first order approximation, simulation of camera rotation and Newton-Raphson type iterations, and give numerical examples for synthetic images. Good results are obtained even for a very sparse texture, and the estimation approaches the true value as the texture density increases.

Lastly, our formulation is compared with those of Aloimonos and Swain [8] and Dunn[9]. Our formulation is general enough to explain their methods in our terms.

Various aspects related to applications and implementations of our method are also discussed.

## 2. TEXTURE DENSITY AND HOMOGENEITY

We consider, in this section, how to define the *density* of a discrete texture. Consider textures composed of dots or line segments. If we are to seek a function  $f(x,y)$  describing the amount of texture divided by the area occupied, we are forced to consider delta-function-like singularities, the value of  $f(x,y)$  being infinity at the texture elements and 0 elsewhere, since the area of a dot or a line segment is 0. This kind of singularities make analytical treatment very difficult. One way to avoid singularities is to regard the texture density as a *functional*.

### DIRAC DELTA FUNCTION

Let us recall the definition of the (Dirac) delta function  $\delta(x)$ . To be precise, it is not a function; if a function takes the value zero except at one point, its integral must be 0, since one point is of Lebesgue measure 0. Instead, consider a *linear functional*  $T$  mapping a smooth (say  $C^\infty$ ) *test function*  $m(x)$  having a finite support (i.e., the domain where it takes non-zero values) to the value  $m(0)$ , i.e.  $T[m(x)] = m(0)$ . This functional is a well defined entity. Now, let us agree to adopt a new *notation* to express the functional; write  $\int \delta(x)(\cdot)dx$ , instead of  $T[\cdot]$ . As a result, the above definition is rewritten as  $\int \delta(x)m(x)dx = m(0)$ . Thus, the delta function is nothing but a *notation* for a special functional. In fact, we do not use the delta function by itself. It is useful in engineering problems only when it is multiplied by some function and integrated. Hence, it suffices to define only the *rule of integration*; we need not worry about its singularity. This is the view developed in detail by Schwartz in his *theory of distributions* [10, 11].

### TEXTURE DENSITY AS A FUNCTIONAL

We fix a *window*  $W$  on the textured image and define the texture density  $f(x,y)$  of a dot texture over the window  $W$  as follows:

**Definition 2.1** (Dot Density). The texture density  $f(x,y)$  of a dot texture over the window  $W$  is a linear functional over a set  $M$ , yet to be specified, of test functions  $m(x,y)$  defined formally by

$$\int_W f(x,y)m(x,y)dxdy = \sum_{P_i \in W} m(x_i, y_i), \quad (2.1)$$

where  $P_i(x_i, y_i)$  are the dot texture elements on the image plane.

Since the texture density is defined as a functional, we need not worry about the singularities of  $f(x,y)$ . We can just *imagine* that  $f(x,y)$  takes the value infinity at texture elements and 0 elsewhere. All we need is the rule of integration. The texture density of a line segment texture is similarly defined as follows:

**Definition 2.2** (Line Segment Density). The texture density  $f(x,y)$  of a line segment texture in the window  $W$  is a linear functional over a set  $M$ , yet to be specified, of test

functions  $m(x,y)$  defined formally by

$$\int_W f(x,y)m(x,y)dxdy = \sum_{L_i \subset W} \int_{L_i} m(x,y)\sqrt{dx^2+dy^2}, \quad (2.2)$$

where  $L_i$  are the line segments on the image plane, and the right-hand side is the sum of line integrals along each line segment.

Here again, we can imagine that  $f(x,y)$  takes the value infinity along texture line segments and 0 elsewhere.

#### HOMOGENEITY

Now, we are in a position to define *homogeneity* of the texture density. Let  $f(x,y)$  be the texture density defined above. We would like to say that the texture is homogeneous if  $f(x,y) \approx c$ , but again, due to singularities, this must be interpreted *in the weak sense* or *in the sense of a distribution*. Namely, let us agree that what we mean by this is as follows:

**Definition 2.3** (Homogeneity). A texture density  $f(x,y)$  is *homogeneous* if

$$\int_W f(x,y)m(x,y)dxdy \approx c \int_W m(x,y)dxdy, \quad (2.3)$$

for test functions  $m(x,y)$  of the set  $M$ , yet to be specified, where  $c$  is a constant independent of the test functions  $m(x,y)$ .

The constant  $c$  can be interpreted as the *texture density* in an intuitive sense, i.e., the "number of dots per unit area" or the "length of line segments per unit area". If we use the definitions of eqns (2.1) and (2.2), our definition is restated as follows.

**Lemma 2.1.** If the texture density is homogeneous, we have the following approximation to integration:

$$\int_W m(x,y)dxdy \approx \begin{cases} \frac{1}{c} \sum_{P_i \in W} m(x_i, y_i) & \text{for dot textures} \\ \frac{1}{c} \sum_{L_i \subset W} \int_{L_i} m(x,y)\sqrt{dx^2+dy^2} & \text{for line segment textures} \end{cases} \quad (2.4)$$

Eqn (2.4) can be viewed as the *Monte Carlo simulation* of integration of a test function  $m(x,y)$ , where  $1/c$  is the "area per dot" or the "area per unit length line segment". The interpretation is that the texture is so homogeneous that the Monte Carlo simulation of integration with respect to the texture elements yields a good approximation.

**Remark 2.1.** If we choose as a test function  $m(x,y)$  the characteristic function

$$\chi_S(x,y) = \begin{cases} 1 & (x,y) \in S \\ 0 & \text{otherwise} \end{cases} \quad (2.5)$$

of a region  $S$ , eqn (2.4) states that the number of dots or the length of line segments in the region  $S$  is approximately proportional to the area of the region  $S$  and that the

constant  $c$  is the number or the length of texture elements in the region  $S$  divided by its area. This is the interpretation which most people informally think of as the definition of homogeneity (cf. the method of Aloimonos and Swain [8] recapitulated in Section 9).

**Remark 2.2** We must mention here that the definition of homogeneity defined above depends on the choice of the set  $M$  of test functions  $m(x,y)$ . Even if the texture is not very dense, it can be homogeneous for very smooth test functions  $m(x,y)$  (i.e., viewed *macroscopically*). However, it may not be homogeneous for rapidly varying test functions  $m(x,y)$  (i.e., viewed *microscopically*). Figuratively speaking, we are looking at the singular texture density  $f(x,y)$  through *filters*  $m(x,y)$ , and the homogeneity is affected by the "coarseness" of the filter through which we are looking. If, for example, we take  $M = \{\exp i\pi(kx/a + ly/b)\}$ , assuming that the window  $W$  is a rectangle of size  $2a \times 2b$ , and set a certain threshold for the approximation of eqn (2.3), we can define the *degree of homogeneity* by those  $(k,l)$  satisfying the approximation. However, we do not go into the details, since what we have described so far is sufficient for the discussion to follow.

## CHANGE OF VARIABLES

Since the integration over the texture is defined as a functional by eqns (2.1) and (2.2), we must be careful when we change the variables of integration. The rule for the usual integration does not apply here. Consider two smooth functions  $u(x,y)$ ,  $v(x,y)$  such that the correspondence between  $(x,y)$  and  $(u,v)$  is one-to-one, and let  $x(u,v)$ ,  $y(u,v)$  be the inverse. Suppose we use  $(u,v)$  as new coordinates. Let  $\tilde{W}$  be the domain on the  $uv$ -plane corresponding to the window  $W$  on the  $xy$ -plane. Define the transformed texture density  $\tilde{f}(u,v)$  also as a functional by

$$\int_{\tilde{W}} \tilde{f}(u,v) \tilde{m}(u,v) du dv = \int_W f(x,y) m(x,y) dx dy, \quad (2.6)$$

where function  $\tilde{m}(u,v)$  is defined by  $\tilde{m}(u,v) \equiv m(x(u,v), y(u,v))$ . Now, consider how the new density  $\tilde{f}(u,v)$  acts, as a functional, on a given test function  $\tilde{m}(u,v)$ .

First, consider a dot texture. Let points  $\tilde{P}_i(u_i, v_i)$  on the  $uv$ -plane be the images of points  $P_i$  on the  $xy$ -plane. Then,

$$\int_W f(x,y) m(x,y) dx dy = \sum_{P_i \in W} m(x_i, y_i) = \sum_{\tilde{P}_i \in \tilde{W}} m(x(u_i, v_i), y(u_i, v_i)) = \sum_{\tilde{P}_i \in \tilde{W}} \tilde{m}(u_i, v_i). \quad (2.7)$$

This relation defines the action of density  $\tilde{f}(u,v)$ , as a functional, on the test function  $\tilde{m}(u,v)$ .

Next, consider a line segment texture. Let  $\tilde{L}_i$  be the line segments on the  $uv$ -plane corresponding to the line segments  $L_i$  on the  $xy$ -plane. Then,

$$\begin{aligned} \int_W f(x,y) m(x,y) dx dy &= \sum_{L_i \subset W} \int_{L_i} m(x,y) \sqrt{dx^2 + dy^2} \\ &= \sum_{\tilde{L}_i \subset \tilde{W}} \int_{\tilde{L}_i} m(x(u,v), y(u,v)) \sqrt{(x_u^2 + y_u^2) \dot{u}^2 + 2(x_u x_v + y_u y_v) \dot{u} \dot{v} + (x_v^2 + y_v^2) \dot{v}^2} \\ &= \sum_{\tilde{L}_i \subset \tilde{W}} \int_{\tilde{L}_i} \tilde{m}(u,v) \frac{\sqrt{(x_u^2 + y_u^2) \dot{u}^2 + 2(x_u x_v + y_u y_v) \dot{u} \dot{v} + (x_v^2 + y_v^2) \dot{v}^2}}{\sqrt{\dot{u}^2 + \dot{v}^2}} \sqrt{du^2 + dv^2}. \end{aligned} \quad (2.8)$$

Here,  $x_u = \partial x(u,v) / \partial u$ , etc., and  $\dot{u} = du(t)/dt$ ,  $\dot{v} = dv(t)/dt$ , where  $(u(t), v(t))$  is an arbitrary

parameterization of individual line segments. Eqn (2.8) defines the action of density  $f(u,v)$ , as a functional, on the test function  $\tilde{m}(u,v)$ . Hence, we conclude as follows.

**Proposition 2.1** (Density Transformation). The transformed texture density  $\tilde{f}(u,v)$  is formally given by

$$\tilde{f}(u,v) = \begin{cases} f(x(u,v), y(u,v)) & \text{for dot textures} \\ f(x(u,v), y(u,v)) \frac{\sqrt{(x_u^2 + y_u^2)u^2 + 2(x_u x_v + y_u y_v)uv + (x_v^2 + y_v^2)v^2}}{\sqrt{u^2 + v^2}} & \text{for line segment textures} \end{cases}, \quad (2.9)$$

where its action as a functional is defined by eqns (2.7) and (2.8).

**Remark 2.3.** For the usual integration of a continuous density, we would have

$$\int_W f(x,y) m(x,y) dx dy = \int_W f(x(u,v), y(u,v)) m(x(u,v), y(u,v)) \begin{vmatrix} x_u & x_v \\ y_u & y_v \end{vmatrix} du dv, \quad (2.10)$$

so that we would obtain

$$\tilde{f}(u,v) = f(x(u,v), y(u,v)) \begin{vmatrix} x_u & x_v \\ y_u & y_v \end{vmatrix}. \quad (2.11)$$

In sum, a continuous density is multiplied by the *Jacobian*, which is the magnification ratio of "area", whereas a line segment density is multiplied by the elongation ratio of "length", which depends on the orientation of individual line segments, and a dot density is multiplied by the increase ratio of "number", which is always unity, since the number of dots is preserved by a continuous mapping.

### 3. FIRST FUNDAMENTAL FORM

In this section, we describe the 3D shape of a surface in the scene in terms of the image coordinates obtained through perspective projection.

#### PERSPECTIVE PROJECTION

Let us fix a Cartesian  $xyz$ -coordinate system in the scene. Let the  $z$ -axis be the optical axis of the camera, and  $(0,0,-f)$ , the point on the  $z$ -axis at distance  $f$  from the  $xy$ -plane, be the focal point. We adopt the camera model that a point in the scene is projected to the intersection of the  $xy$ -plane with the ray connecting the point and the focal point (Fig. 1). Thus, the  $xy$ -plane plays the role of the image plane and  $f$  is the *focal length*. It is easily seen from Fig. 1 that the correspondence between the point  $(X,Y,Z)$  in the scene and the projected point  $(x,y)$  on the image plane is given by

$$x = \frac{fX}{f+Z}, \quad y = \frac{fY}{f+Z}. \quad (3.1)$$

#### SURFACE DIFFERENTIALS

Consider a smooth surface in the scene whose equation is  $Z=Z(X,Y)$ . This equation coupled with eqns (3.1) determines a one-to-one correspondence between the points in the scene and the points on the image plane in the form of  $X=X(x,y)$ ,  $Y=Y(x,y)$ . We

first study how the space coordinates  $X, Y, Z$  change on the surface by considering the relationship among differentials  $dX, dY, dZ$  taken along the surface. Taking the differentials of both sides of eqns (3.1), we obtain

$$fdX - x dZ = (f + Z) dx, \quad fdY - y dZ = (f + Z) dy. \quad (3.2)$$

Taking the differentials of both sides of  $Z = Z(X, Y)$ , we obtain

$$dZ = P dX + Q dY \quad (P \equiv \partial Z / \partial X, \quad Q \equiv \partial Z / \partial Y). \quad (3.3)$$

Eqns (3.2) and (3.3) can be viewed as a set of simultaneous linear equations in  $dX, dY, dZ$ . The solution is obtained in the form

$$\begin{aligned} dX &= \frac{f+Z}{f(f-Px-Qy)} [(f-Qy)dx + Qx dy], \\ dY &= \frac{f+Z}{f(f-Px-Qy)} [Py dx + (f-Px) dy], \\ dZ &= \frac{f+Z}{f-Px-Qy} [P dx + Q dy]. \end{aligned} \quad (3.4)$$

Here, all the quantities on the right-hand sides are viewed as functions of the image coordinates  $x, y$  through

$$Z = Z(X(x, y), Y(x, y)), \quad P = \frac{\partial Z}{\partial X}(X(x, y), Y(x, y)), \quad Q = \frac{\partial Z}{\partial Y}(X(x, y), Y(x, y)). \quad (3.5)$$

#### FIRST FUNDAMENTAL FORM

Consider two points  $(x, y), (x+dx, y+dy)$  infinitesimally far apart on the image plane. Let  $ds$  be the 3D distance between the corresponding points on the surface. Since  $ds^2 = dX^2 + dY^2 + dZ^2$ , substitution of eqns (3.4) yields

**Proposition 3.1** (First Fundamental Form).

$$ds^2 = \sum_{i,j=1}^2 g_{ij} dx^i dx^j, \quad (3.6)$$

where  $x^1 = x, x^2 = y$  and

$$\begin{aligned} g_{11}(x, y) &= \frac{(1+Z/f)^2}{(1-(Px+Qy)/f)^2} [(1+P^2) - 2Qy/f + (P^2+Q^2)y^2/f^2], \\ g_{12}(x, y) &= \frac{(1+Z/f)^2}{(1-(Px+Qy)/f)^2} [PQ + (Qx+Py)/f - (P^2+Q^2)xy/f^2] = g_{21}(x, y), \\ g_{22}(x, y) &= \frac{(1+Z/f)^2}{(1-(Px+Qy)/f)^2} [(1+Q^2) - 2Px/f + (P^2+Q^2)x^2/f^2]. \end{aligned} \quad (3.7)$$

Eqn (3.7) is called the *first fundamental form* and  $g = (g_{ij})$  is called the *first fundamental metric tensor*. The first fundamental form of eqn (3.7) indeed plays a fundamental role in computing 3D quantities in terms of the image coordinates. For example, consider an arbitrary smooth curve  $L$  on the image plane. The true arc length of the

corresponding curve on the surface is given by integration  $\int_L ds = \int_L \sqrt{\sum_{i,j=1}^2 g_{ij} dx^i dx^j}$  on the image plane.

Consider an infinitesimally small square on the image plane defined by four points  $(x, y)$ ,  $(x+dx, y)$ ,  $(x, y+dy)$ ,  $(x+dx, y+dy)$ . The area of this square on the image plane is  $dx dy$ , but it is easy to show that the true area of the corresponding region of the surface is given by  $\sqrt{\det(g)} dx dy$ . From eqns (3.8), we obtain

$$\sqrt{\det(g)} = \frac{\sqrt{1+P^2+Q^2}(1+Z/f)^2}{1-(Px+Qy)/f}. \quad (3.9)$$

Hence, the true area of the region of the surface corresponding to a region  $S$  of the image plane is given by integration  $\int_S \sqrt{\det(g)} dx dy$  on the image plane.

The first fundamental form makes it possible to express various other 3D geometrical properties such as angle, Levi-Civita parallelism, geodesics and surface gradient in terms of the image coordinates (Appendix A).

#### PLANAR SURFACES

If the surface is a plane given by equation  $Z = pX + qY + r$ , where  $p, q, r$  are constants, eqns (3.1) can be solved for  $X, Y$  in the form

$$X = \frac{(f+r)x}{f-px-xy}, \quad Y = \frac{(f+r)y}{f-px-xy}, \quad Z = \frac{f(px+qy+r)}{f-px-xy}. \quad (3.10)$$

Since  $1+Z/f = (1+r/f)/(1-(px+qy)/f)$ , eqns (3.8) and eqn (3.9) become as follows:

$$\begin{aligned} g_{11}(x, y) &= \frac{(1+r/f)^2}{(1-(px+qy)/f)^4} [1+p^2-2qy/f+(p^2+q^2)y^2/f^2], \\ g_{12}(x, y) &= \frac{(1+r/f)^2}{(1-(px+qy)/f)^4} [pq+(qx+py)/f-(p^2+q^2)xy/f^2] = g_{21}(x, y), \\ g_{22}(x, y) &= \frac{(1+r/f)^2}{(1-(px+qy)/f)^4} [1+q^2-2px/f+(p^2+q^2)x^2/f^2], \end{aligned} \quad (3.11)$$

$$\sqrt{\det(g)} = \frac{\sqrt{1+p^2+q^2}(1+r/f)^2}{(1-(px+qy)/f)^3}. \quad (3.12)$$

#### 4. RECOVERY OF PLANAR SURFACE ORIENTATION FROM TEXTURE

In this section, we consider a principle to compute the surface shape by observing an inhomogeneous texture density  $f(x, y)$  on the assumption that the true texture is homogeneous. We must first study what  $f(x, y)$  looks like if the true texture is homogeneous. Since the texture density is defined as a functional, what we need to know is how the observed density  $f(x, y)$  acts on a test function  $m(x, y)$  as a functional. Then, we derive the basic equations to determine the surface shape in term of *observables* computed on the image plane.

##### DISTORTION OF HOMOGENEOUS TEXTURE

Consider temporarily a curvilinear coordinate system  $(u, v)$  on the surface and assume a one-to-one correspondence  $u = u(x, y)$ ,  $v = v(x, y)$  and  $x = x(u, v)$ ,  $y = y(u, v)$ . Let  $W_0$  be the region of the surface corresponding to the window  $W$  on the image plane. Let

$f_0(u, v)$  be the homogeneous texture density defined on the surface, and let  $m_0(u, v) \equiv m(x(u, v), y(u, v))$ . According to the assumption of homogeneity, we have

$$\int_{W_0} f_0(u, v) m_0(u, v) dS_0 \approx c \int_{W_0} m_0(u, v) dS_0, \quad (4.1)$$

where  $dS_0$  is the area element of the surface.

Consider how eqn (4.1) is expressed in terms of the image coordinates  $x, y$ . Since the right-hand side is the usual integration and  $dS_0 = \sqrt{\det(g)} dx dy$ , it becomes

$$c \int_W m(x, y) \sqrt{\det(g)} dx dy. \quad (4.2)$$

The transformation of the left-hand side depends on whether the texture consists of dots or line segments.

For a dot texture, the right-hand side is written, according to Proposition 2.1, as

$$\sum_{P \in W} m(x_i, y_i) (= \int_W f(x, y) m(x, y) dx dy), \quad (4.3)$$

which can be computed readily on the image plane.

For a line segment texture, the right-hand side is written, in view of Proposition 2.1 and  $ds = \sqrt{\sum_{i,j=1}^2 g_{ij} dx^i dx^j}$ , as

$$\sum_{L \subset W} \int_L m(x, y) \Gamma(x, y) \sqrt{dx^2 + dy^2}, \quad (4.4)$$

where

$$\Gamma(x, y) \equiv \frac{\sqrt{g_{11}x^2 + 2g_{12}xy + g_{22}y^2}}{\sqrt{x^2 + y^2}} \quad (4.5)$$

is the elongation ratio of the line segment at  $(x, y)$ , which depends on the orientation of the line segment.

The difficulty is that we cannot compute this integral on the image plane unless we know the first fundamental form, which is dependent of the surface shape. Here, we adopt the approximation

$$\Gamma(x, y) \approx (\sqrt{\det(g)})^{1/2}. \quad (4.6)$$

The interpretation is that the line segments are distributed nearly isotropically, so that if the area is enlarged  $\sqrt{\det(g)}$  times, the individual line segments become roughly  $(\sqrt{\det(g)})^{1/2}$  times as long. Then, regarding  $m(x, y)\Gamma(x, y)$  as a new test function  $m(x, y)$ , we can treat both dot textures and line segment textures in the same way. Namely, if we compute, as an *observable*, integration

$$J = \int_W f(x, y) m(x, y) dx dy \quad (4.7)$$

of a test function  $m(x, y)$  over the window  $W$ , we obtain the relation

$$J \approx c \int_W m(x, y) (\sqrt{\det(g)})^\kappa dx dy, \quad (4.8)$$

where  $\kappa=1$  for a dot texture and  $\kappa=1/2$  for a line segment texture.

**Remark 4.1.** Eqn (4.8) is interpreted intuitively as follows. Consider a small region  $S$  on the image plane, and let  $S_0$  be the corresponding region on the surface. For a dot

texture, the number of dots in  $S$  is equal to the number of dots in  $S_0$ , while the area of  $S$  is  $1/\sqrt{\det(g)}$  times that of  $S_0$ . Hence, the texture density in  $S$  is  $\sqrt{\det(g)}$  times that in  $S_0$ . For a line segment texture, if the true texture is nearly isotropic, the total length of the line segments in  $S$  is approximately  $1/(\sqrt{\det(g)})^{1/2}$  times that of  $S_0$ . Since the area of  $S$  is  $1/\sqrt{\det(g)}$  times that of  $S_0$ , the texture density in  $S$  is  $(\sqrt{\det(g)})^{1/2}$  times that in  $S_0$ .

## GENERAL PRINCIPLE OF SURFACE RECOVERY

Our principle of surface recovery is as follows. Let the object surface be parameterized so that the procedure reduces to parameter estimation. Then, the right-hand side of eqn (4.8) is a known form in unknown parameters. If we appropriately provide test functions  $m_0(x,y)$ ,  $m_1(x,y)$ ,  $m_2(x,y)$ , ..., we can compute the corresponding *observables*  $J_0$ ,  $J_1$ ,  $J_2$ , ... by summation or integration on the image plane. As a result, the necessary number of equations are obtained in the form of eqn (4.8) to determine the parameter values.

## BASIC EQUATIONS FOR PLANAR SURFACES

The simplest case is when the surface is a plane. If we replace the approximate equality in eqn (4.8) by equality, assuming that the true texture is sufficiently homogeneous, we obtain from eqn (3.12)

$$J = c(\sqrt{1+p^2+q^2})^\kappa (1+\frac{r}{f})^{2\kappa} \int_W \frac{m(x,y) dx dy}{(1-(px+qy)/f)^{3\kappa}}. \quad (4.9)$$

Now, provide three test functions  $m_0(x,y)$ ,  $m_1(x,y)$ ,  $m_2(x,y)$ , and let  $J_i$ ,  $i=0,1,2$ , be the corresponding observables. If we consider ratios  $J_1/J_0$ ,  $J_2/J_0$ , dropping off the common factor  $c(\sqrt{1+p^2+q^2})^\kappa (1+r/f)^{2\kappa}$ , we obtain the following equations.

**Proposition 4.1** (Basic Equations). The surface gradient  $(p,q)$  is determined by solving

$$\int_W \frac{m_i(x,y) - (J_i/J_0)m_0(x,y)}{(1-(px+qy)/f)^{3\kappa}} dx dy = 0, \quad i=1,2. \quad (4.10)$$

**Remark 4.2.** Eqns (4.10) are the basic equations to determine  $(p,q)$  and can be solved in principle, say by iterative search in the  $pq$ -space. Evidently, three test functions are enough to determine the surface gradient. However, we can also employ many more test functions and determine  $(p,q)$  by some fitting scheme (cf. the method of Dunn [9] recast in Section 9).

## SMALL GRADIENT APPROXIMATION

Suppose the surface gradient  $(p,q)$  is close to zero compared with the focal length  $f$  of the camera, so that  $px+qy \ll f$  in the window  $W$ . Since  $px+qy=f$  is the *vanishing line* or "horizon" of the surface ( $\sqrt{\det(g)}$  of eqn (3.12) becomes  $\infty$  there), our assumption is that the image in the window  $W$  is not near the vanishing line. (If the vanishing line happens to be observed on the image plane, its equation  $px+qy=f$  immediately tells us the gradient  $(p,q)$ .) If  $px+qy \ll f$ , the Taylor expansion around the origin yields

$$\frac{1}{(1-(px+qy)/f)^{3\kappa}} = 1 + \frac{3\kappa}{f}(px+qy) + \dots \quad (4.11)$$

If we put

$$L_i = \int_W m_i(x,y) dx dy, \quad M_i = \int_W x m_i(x,y) dx dy, \quad N_i = \int_W y m_i(x,y) dx dy \quad (4.12)$$

for  $i=0,1,2$  and neglect higher order terms, the basic equations (4.10) reduce to the following linear equations in  $p, q$ :

$$\begin{bmatrix} M_1 - (J_1/J_0)M_0 & N_1 - (J_1/J_0)N_0 \\ M_2 - (J_2/J_0)M_0 & N_2 - (J_2/J_0)N_0 \end{bmatrix} \begin{bmatrix} p \\ q \end{bmatrix} = -\frac{f}{3\kappa} \begin{bmatrix} L_1 - (J_1/J_0)L_0 \\ L_2 - (J_2/J_0)L_0 \end{bmatrix} \quad (4.13)$$

A simple choice of the test functions  $m_i(x,y)$ ,  $i=0,1,2$  is

$$m_0(x,y)=1, \quad m_1(x,y)=x, \quad m_2(x,y)=y. \quad (4.14)$$

Then,  $J_1/J_0$ ,  $J_2/J_0$  are nothing but the coordinates of the *center of gravity* of the texture inside the window  $W$ . If the window  $W$  is a rectangle defined by  $-a \leq x \leq a$ ,  $-b \leq y \leq b$ , the solution of eqns (4.13) is written as

$$p = \sqrt{x}/\kappa a^2, \quad q = \sqrt{y}/\kappa b^2, \quad (4.15)$$

where  $(\bar{x}, \bar{y})$  is the center of gravity of the texture in the window  $W$ . If  $(p,q)=(0,0)$ , i.e., if the surface is viewed orthogonally, the center of gravity of the texture coincides with the origin. Otherwise, the orientation and the magnitude of the "shift" of the center of gravity of the texture gives the surface gradient  $(p,q)$ .

**Remark 4.3** The accuracy of the result depends on both the number or length of the texture elements observed in the window  $W$  and the distribution pattern of those texture elements. Let  $N$  be the number or the length of the texture elements in the window  $W$ . The rule of thumb is that the error is approximately proportional to  $1/\sqrt{N}$  when the texture is completely random and is approximately proportional to  $1/N$  when the texture is very regular and periodic (cf. Appendix A). Textures we often encounter in natural scenes and man-made objects are usually regular and periodic "tessellations", for which high accuracy is expected.

## 5. SCHEME OF ITERATIVE CORRECTION FOR PLANAR SURFACES

The method in the previous section is based on the assumption that the gradient  $(p,q)$  is close to zero. There exist methods which can be applied when the gradient is not small. The first method is based on the following observation.

### GENERAL PRINCIPLE

Suppose the camera is rotated by a certain angle around its focus relative to a stationary scene. As a result, a different image is seen on the image plane. However, since a point on the image plane actually corresponds to a "ray" in the 3D scene, occlusion is not affected by camera rotation. If the angle of camera rotation is known, the original image can be recovered as long as the effect of the image boundary is not involved. An important fact is that the image transformation due to camera rotation *does not require any knowledge of the 3D scene*.

Suppose the camera is rotated by an orthogonal matrix  $R=(r_{ij})$ . The rotation of the camera by  $R$  is equivalent to the rotation of the scene by  $R^{-1}(=R^T)$ . By rotation  $R^T$ , a point  $(X, Y, Z)$  moves to a point  $(\tilde{X}, \tilde{Y}, \tilde{Z})$ , where

$$\begin{bmatrix} \tilde{X} \\ \tilde{Y} \\ f+\tilde{Z} \end{bmatrix} = \begin{bmatrix} r_{11} & r_{21} & r_{31} \\ r_{12} & r_{22} & r_{32} \\ r_{13} & r_{23} & r_{33} \end{bmatrix} \begin{bmatrix} X \\ Y \\ f+Z \end{bmatrix}. \quad (5.1)$$

This point is projected onto  $(\tilde{x}, \tilde{y})$  on the image plane, where  $\tilde{x}=f\tilde{X}/(f+\tilde{Z})$ ,  $\tilde{y}=f\tilde{Y}/(f+\tilde{Z})$ . Combining this with eqns (3.1), we obtain the transformation rule

$$\tilde{x} = f \frac{r_{11}x + r_{21}y + r_{31}f}{r_{13}x + r_{23}y + r_{33}f}, \quad \tilde{y} = f \frac{r_{12}x + r_{22}y + r_{32}f}{r_{13}x + r_{23}y + r_{33}f}. \quad (5.2)$$

Suppose the surface gradient is not small. We first apply the method in the previous section. Let  $(\bar{p}, \bar{q})$  be the computed gradient. This estimation may not be accurate. Now, suppose the camera is rotated in such a way that the estimated surface becomes parallel to the image plane. As a result, the gradient of the true surface becomes small, so that the method in the previous section can be applied again. Let  $(\tilde{p}, \tilde{q})$  be the computed gradient. If this newly estimated surface is rotated back into the original camera orientation, the obtained gradient  $(p', q')$  must be a better estimate. This process can be applied repeatedly until no further improvement is obtained. This is the basic concept of the iterative correction scheme by camera rotation.

We should note first that *the camera need not actually be rotated*. Since the image transformation due to camera rotation is given by eqns (5.2), the transformed image  $\tilde{f}(\tilde{x}, \tilde{y})$  can be obtained by computation. However, we should also note that *the transformed image need not actually be computed*. This is because all we need to do is apply appropriate test functions  $m(\tilde{x}, \tilde{y})$  and integrate them over the image. Since the transformation is explicitly given by eqns (5.2), the variables of integration can be changed so that the integration can be done over the original image. In other words, instead of integrating the test functions  $m(\tilde{x}, \tilde{y})$  over the transformed image  $\tilde{f}(\tilde{x}, \tilde{y})$ , we can equivalently integrate the transformed test functions  $\tilde{m}(x, y)$  over the original image  $f(x, y)$ . Consequently, our iterative correction scheme is performed by iteratively modifying the test functions, not the image.

#### CAMERA ROTATION SIMULATION

Let  $(\bar{p}, \bar{q})$  be the initial estimate of the gradient. In terms of the surface unit normal vector  $\mathbf{n}=(n_1, n_2, n_3)$ , this means

$$n_1 = -\frac{\bar{p}}{\sqrt{1+\bar{p}^2+\bar{q}^2}}, \quad n_2 = -\frac{\bar{q}}{\sqrt{1+\bar{p}^2+\bar{q}^2}}, \quad n_3 = \frac{1}{\sqrt{1+\bar{p}^2+\bar{q}^2}}. \quad (5.3)$$

This vector makes angle

$$\Omega = \cos^{-1} n_3 \quad (5.4)$$

with the unit vector  $\mathbf{k}=(0,0,1)$  along the  $z$ -axis. The unit vector normal to both  $\mathbf{n}$  and  $\mathbf{k}$  is given by

$$l = \frac{\mathbf{k} \times \mathbf{n}}{\|\mathbf{k} \times \mathbf{n}\|} = \frac{(\bar{q}, -\bar{p}, 0)}{\sqrt{\bar{p}^2 + \bar{q}^2}}. \quad (5.5)$$

If the camera is rotated around the vector  $l$  by angle  $\Omega$  screwwise, the estimated surface becomes parallel to the image plane. The corresponding rotation matrix is given by

$$R = \begin{bmatrix} r_{11} & r_{12} & n_1 \\ r_{12} & r_{22} & n_2 \\ -n_1 & -n_2 & n_3 \end{bmatrix}, \quad (5.6)$$

where

$$r_{11} = \frac{\bar{p}^2 n_3 + \bar{q}^2}{\bar{p}^2 + \bar{q}^2}, \quad r_{12} = \frac{\bar{p}\bar{q}(n_3 - 1)}{\bar{p}^2 + \bar{q}^2}, \quad r_{22} = \frac{\bar{q}^2 n_3 + \bar{p}^2}{\bar{p}^2 + \bar{q}^2}. \quad (5.7)$$

Hence, the image transformation is given by

$$\tilde{x}(x, y) = f \frac{r_{11}x + r_{12}y - n_1 f}{n_1 x + n_2 y + n_3 f}, \quad \tilde{y}(x, y) = f \frac{r_{12}x + r_{22}y - n_2 f}{n_1 x + n_2 y + n_3 f}, \quad (5.8)$$

and its Jacobian is

$$J(x, y) = \begin{vmatrix} \tilde{x}_x & \tilde{x}_y \\ \tilde{y}_x & \tilde{y}_y \end{vmatrix} = -f \frac{n_1 \tilde{x}(x, y) + n_2 \tilde{y}(x, y) - n_3 f}{(n_1 x + n_2 y + n_3 f)^2}. \quad (5.9)$$

The transformation of eqns (5.8) maps the origin (0,0) into point  $(f\bar{p}, f\bar{q})$ . If the original image is restricted to a window  $W$  around the origin, the transformed image is also restricted to the corresponding domain  $\tilde{W}$  around point  $(f\bar{p}, f\bar{q})$ . Let  $(\bar{p}, \bar{q})$  be the true gradient of the transformed surface. The Taylor expansion around point  $(f\bar{p}, f\bar{q})$  yields

$$\frac{1}{(1 - (\tilde{p}\tilde{x} + \tilde{q}\tilde{y})/f)^{3\kappa}} = \frac{1}{(1 - \bar{p}\bar{p} - \bar{q}\bar{q})^{3\kappa}} (1 + A(\tilde{x} - f\bar{p}) + B(\tilde{y} - f\bar{q}) + \dots), \quad (5.10)$$

where

$$A = \frac{3\kappa\bar{p}}{f(1 - \bar{p}\bar{p} - \bar{q}\bar{q})}, \quad B = \frac{3\kappa\bar{q}}{f(1 - \bar{p}\bar{p} - \bar{q}\bar{q})}. \quad (5.11)$$

If eqns (5.10) are substituted, the basic equations (4.10) become

$$\begin{bmatrix} \tilde{M}_1 - (\tilde{J}_1/\tilde{J}_0)\tilde{M}_0 & \tilde{N}_1 - (\tilde{J}_1/\tilde{J}_0)\tilde{N}_0 \\ \tilde{M}_2 - (\tilde{J}_2/\tilde{J}_0)\tilde{M}_0 & \tilde{N}_2 - (\tilde{J}_2/\tilde{J}_0)\tilde{N}_0 \end{bmatrix} \begin{bmatrix} A \\ B \end{bmatrix} = - \begin{bmatrix} \tilde{L}_1 - (\tilde{J}_1/\tilde{J}_0)\tilde{L}_0 \\ \tilde{L}_2 - (\tilde{J}_2/\tilde{J}_0)\tilde{L}_0 \end{bmatrix}, \quad (5.12)$$

where

$$\tilde{J}_i = \int_{\tilde{W}} m_i(\tilde{x}, \tilde{y}) \tilde{f}(\tilde{x}, \tilde{y}) d\tilde{x} d\tilde{y}, \quad (5.13)$$

$$\tilde{L}_i = \int_{\tilde{W}} m_i(\tilde{x}, \tilde{y}) d\tilde{x} d\tilde{y}, \quad \tilde{M}_i = \int_{\tilde{W}} (\tilde{x} - f\bar{p}) m_i(\tilde{x}, \tilde{y}) d\tilde{x} d\tilde{y}, \quad \tilde{N}_i = \int_{\tilde{W}} (\tilde{y} - f\bar{q}) m_i(\tilde{x}, \tilde{y}) d\tilde{x} d\tilde{y}, \quad (5.14)$$

and  $\tilde{f}(\tilde{x}, \tilde{y})$  is the transformed texture density.

Once  $A, B$  are determined by solving eqn (5.12), the gradient  $(\bar{p}, \bar{q})$  are determined by solving eqns (5.11), which are rewritten as

$$\begin{bmatrix} A\bar{p}+3\kappa/f & A\bar{q} \\ B\bar{p} & B\bar{q}+3\kappa/f \end{bmatrix} \begin{bmatrix} \bar{p} \\ \bar{q} \end{bmatrix} = \begin{bmatrix} A \\ B \end{bmatrix}. \quad (5.15)$$

If the computed gradient  $(pt, \bar{q})$  is sufficiently close to zero, the initial estimate is correct. Otherwise, the camera is rotated back into the original orientation, and the surface gradient is transformed into

$$p' = \frac{r_{11}\bar{p}+r_{12}\bar{q}-n_1}{n_1\bar{p}+n_2\bar{q}+n_3}, \quad q' = \frac{r_{12}\bar{p}+r_{22}\bar{q}-n_2}{n_1\bar{p}+n_2\bar{q}+n_3}, \quad (5.16)$$

These values are better approximations to the surface gradient. This process can be iterated by setting  $\bar{p} \leftarrow p'$ ,  $\bar{q} \leftarrow q'$  and repeating the previous procedure until convergence.

#### COMPUTATION ON THE ORIGINAL IMAGE

Consider how to compute eqns (5.13) and (5.14) without actually transforming the image. For a dot texture, we see, from Proposition 2.1, that if we put

$$\tilde{m}_i(x, y) \equiv m_i(\tilde{x}(x, y), \tilde{y}(x, y)), \quad i=0, 1, 2, \quad (5.17)$$

we obtain

$$\tilde{J}_i = \sum_{P \in W} \tilde{m}_i(x_i, y_i). \quad (5.18)$$

Thus, computation can be done on the original image.

For a line segment texture, we also see, from Proposition 2.1, that

$$\tilde{J}_i = \sum_{L \subset W} \int_{L_i} \tilde{m}_i(x, y) \sqrt{E(x, y)dx^2 + 2F(x, y)dx dy + G(x, y)dy^2}, \quad (5.19)$$

where

$$\begin{aligned} E(x, y) &\equiv \tilde{x}_x^2 + \tilde{y}_x^2 = f^2 \frac{1 + n_1^2(\tilde{x}(x, y)^2 + \tilde{y}(x, y)^2 - 1) - 2n_1(r_{11}\tilde{x}(x, y) + r_{12}\tilde{y}(x, y))}{(n_1x + n_2y + n_3f)^2}, \\ F(x, y) &\equiv \tilde{x}_x\tilde{x}_y + \tilde{y}_x\tilde{y}_y \\ &= f^2 \frac{n_1n_2(\tilde{x}(x, y)^2 + \tilde{y}(x, y)^2 - 1) - n_1(r_{12}\tilde{x}(x, y) + r_{22}\tilde{y}(x, y)) - n_2(r_{11}\tilde{x}(x, y) + r_{12}\tilde{y}(x, y))}{(n_1x + n_2y + n_3f)^2}, \\ G(x, y) &\equiv \tilde{x}_y^2 + \tilde{y}_y^2 = f^2 \frac{1 + n_2^2(\tilde{x}(x, y)^2 + \tilde{y}(x, y)^2 - 1) - 2n_2(r_{12}\tilde{x}(x, y) + r_{22}\tilde{y}(x, y))}{(n_1x + n_2y + n_3f)^2}. \end{aligned} \quad (5.20)$$

Thus, computation can be done on the original image.

Eqns (5.14) are, on the other hand, integrations of continuous functions. Hence, we immediately obtain

$$\begin{aligned} \tilde{L}_i &= \int_W \tilde{m}_i(x, y) J(x, y) dx dy, \\ \tilde{M}_i &= \int_W (\tilde{x}(x, y) - f\bar{p}) \tilde{m}_i(x, y) J(x, y) dx dy, \end{aligned} \quad (5.21)$$

$$\bar{N}_i = \int_W (\tilde{y}(x, y) - f\bar{q}) \tilde{m}_i(x, y) J(x, y) dx dy.$$

These are computed by a numerical integration scheme.

**Remark 5.1.** Eqn (5.19) is a rigorous relation. A simple approximation is given, corresponding to eqn (4.6), by

$$\bar{J}_i \approx \sum_{L_i \subset W} \int_{L_i} \tilde{m}_i(x, y) \sqrt{J(x, y)} \sqrt{dx^2 + dy^2}. \quad (5.22)$$

#### ALTERNATIVE METHOD BY TAYLOR EXPANSION

The method described above is somewhat complicated. There exists an alternative scheme whose formulation is simpler. Suppose  $(\bar{p}, \bar{q})$  is an initial estimate. We replace eqn (4.11) with the Taylor expansion with respect to  $(p, q)$  at  $(\bar{p}, \bar{q})$ :

$$\frac{1}{(1-(px+qy)/f)^{3\kappa}} = L(x, y) + M(x, y)\delta p + N(x, y)\delta q + \dots \quad (5.23)$$

Here,  $\delta p = p - \bar{p}$ ,  $\delta q = q - \bar{q}$  and

$$\begin{aligned} L(x, y) &= \frac{1}{(1-(\bar{p}x + \bar{q}y)/f)^{3\kappa}}, \\ M(x, y) &= \frac{3\kappa x}{f(1-(\bar{p}x + \bar{q}y)/f)^{3\kappa+1}}, \\ N(x, y) &= \frac{3\kappa y}{f(1-(\bar{p}x + \bar{q}y)/f)^{3\kappa+1}}. \end{aligned} \quad (5.24)$$

Then, the basic equations (4.10) become

$$\begin{bmatrix} M_1 - (J_1/J_0)M_0 & N_1 - (J_1/J_0)N_0 \\ M_2 - (J_2/J_0)M_0 & N_2 - (J_2/J_0)N_0 \end{bmatrix} \begin{bmatrix} \delta p \\ \delta q \end{bmatrix} = - \begin{bmatrix} L_1 - (J_1/J_0)L_0 \\ L_2 - (J_2/J_0)L_0 \end{bmatrix}, \quad (5.25)$$

where

$$L_i = \int_W m_i(x, y) L(x, y) dx dy, \quad M_i = \int_W m_i(x, y) M(x, y) dx dy, \quad N_i = \int_W m_i(x, y) N(x, y) dx dy, \quad (5.26)$$

for  $i=0, 1, 2$ . If  $\delta p$ ,  $\delta q$  are sufficiently close to zero, the initial estimate is sufficiently accurate. Otherwise,  $p' = \bar{p} + \delta p$ ,  $q' = \bar{q} + \delta q$  are better approximations. This process can be iterated by setting  $\bar{p} \leftarrow p'$ ,  $\bar{q} \leftarrow q'$  and repeating this procedure until convergence.

**Remark 5.2.** This method is essentially the *Newton-Raphson iteration* of the basic equations. Although this method seems simpler, the geometrical meaning of functions  $M(x, y)$ ,  $N(x, y)$  is not clear, while the method of camera rotation has a clear geometrical meaning. In addition, the method of Taylor expansion still involves the approximation (4.6), while the method of camera rotation is not so much affected by that approximation; the texture image is *exactly* transformed (cf. eqns (5.18), (5.19)) repeatedly so that the true surface becomes more and more parallel to the image plane, and in the limit of  $p \rightarrow 0$ ,  $q \rightarrow 0$ , the approximation (4.6) reduces to a trivial identity.

## 6. PRINCIPLE OF CURVED SURFACE RECOVERY FROM TEXTURE

Eqn (4.13) can be applied even if the surface is not planar if we choose windows of an appropriate size so that the surface is approximately planar in each window. Then, eqn (4.13) gives the gradient  $(p, q)$  for each window. Thus, the global 3D shape of an arbitrary smooth surface can be recovered in principle. Another approach to curved surfaces is to use a surface model. Assume, for example, that the equation of the surface is given by

$$Z = r + pX + qY + \alpha X^2 + 2\beta XY + \gamma Y^2. \quad (6.1)$$

### BASIC EQUATIONS FOR CURVED SURFACES

If the surface is planar, the observed texture inhomogeneity is solely due to the perspective distortion, whereas if the surface is curved, the inhomogeneity is due to two separate sources - the perspective distortion and the varying gradient. In other words, inhomogeneity is not observed for planar surfaces if the projection is orthographic, i.e.,  $f \rightarrow \infty$ , while for curved surfaces inhomogeneity results even if the projection is orthographic. Here, let us consider orthographic projection. Letting  $f \rightarrow \infty$ , we obtain  $x = X$ ,  $y = Y$  and

$$\sqrt{\det(g)} = \sqrt{1+p^2+q^2} \sqrt{1+A_1x+A_2y+A_3x^2+2A_4xy+A_5y^2}, \quad (6.2)$$

where

$$\begin{aligned} A_1 &= \frac{4(\alpha p + \beta q)}{1+p^2+q^2}, & A_2 &= \frac{4(\beta p + \gamma q)}{1+p^2+q^2}, \\ A_3 &= \frac{4(\alpha^2 + \beta^2)}{1+p^2+q^2}, & A_4 &= \frac{4\beta(\alpha + \gamma)}{1+p^2+q^2}, & A_5 &= \frac{4(\beta^2 + \gamma^2)}{1+p^2+q^2}. \end{aligned} \quad (6.3)$$

Since  $\sqrt{1+p^2+q^2}$  drops off when the unknown true texture density  $c$  is eliminated, all that can be determined are parameters  $A_i$ ,  $i=1, \dots, 5$ , which we call *texture density parameters*. Consequently, we cannot distinguish surfaces which have the same values for the texture density parameters  $A_i$ ,  $i=1, \dots, 5$ .

If we provide six test functions  $m_0(x, y)$ , ...,  $m_5(x, y)$  and compute as observables

$$J_i = \int_W f(x, y) m_i(x, y) dx dy, \quad i=0, 1, \dots, 5, \quad (6.4)$$

the basic equations are, instead of eqns (4.10), given by

**Proposition 6.1** (Basic Equations). The texture density parameters are determined by solving

$$\int_W (m_i(x, y) - \frac{J_i}{J_0} m_0(x, y)) (\sqrt{1+A_1x+A_2y+A_3x^2+2A_4xy+A_5y^2})^k dx dy = 0, \quad i=1, \dots, 5. \quad (6.5)$$

Thus, six test functions are enough to determine the texture density parameters  $A_i$ ,  $i=1, \dots, 5$ . Of course, we can use many more functions and determine the surface parameters by some fitting scheme.

## INTERPRETATION OF CURVED SURFACES

Once the texture density parameters  $A_i$ ,  $i=1,\dots,5$  are obtained, the surface parameters  $p$ ,  $q$ ,  $\alpha$ ,  $\beta$ ,  $\gamma$  are determined by solving eqns (6.3). The solution is given as follows (see Appendix B for proof).

**Proposition 6.2.** The surface parameters  $p$ ,  $q$ ,  $\alpha$ ,  $\beta$ ,  $\gamma$  are given by

$$p=k\tilde{p}, \quad q=k\tilde{q}, \quad \alpha=k\tilde{\alpha}, \quad \beta=k\tilde{\beta}, \quad \gamma=k\tilde{\gamma}. \quad (6.6)$$

Here,  $\tilde{\alpha}$ ,  $\tilde{\beta}$ ,  $\tilde{\gamma}$  are given by

$$\tilde{\alpha}=\tau+\frac{A_3-A_5}{16\tau}, \quad \tilde{\beta}=\frac{A_4}{8\tau}, \quad \tilde{\gamma}=\tau-\frac{A_3-A_5}{16\tau}, \quad (6.7)$$

where

$$\tau=\pm\frac{1}{4}\sqrt{A_3+A_5\pm2\sqrt{A_3A_5-A_4^2}}. \quad (6.8)$$

Then,  $\tilde{p}$ ,  $\tilde{q}$  are given by

$$\tilde{p}=\frac{\tilde{\gamma}A_1-\tilde{\beta}A_2}{4(\tilde{\alpha}\tilde{\gamma}-\tilde{\beta}^2)}, \quad \tilde{q}=\frac{-\tilde{\beta}A_1+\tilde{\alpha}A_2}{4(\tilde{\alpha}\tilde{\gamma}-\tilde{\beta}^2)}, \quad (6.9)$$

and  $k$  is given by

$$k=\frac{1}{\sqrt{1-\tilde{p}^2-\tilde{q}^2}}. \quad (6.10)$$

## AMBIGUITY OF INTERPRETATION

From eqn (6.8), we see that there exist at most four solutions. This is an essential characteristic of orthographic projection. Firstly, the projected image is not affected if we take the *mirror image* of the surface with respect to a mirror perpendicular to the  $z$ -axis. The four solutions consist of two pairs of mirror images. Another ambiguity occurs because the texture density only tells about the amount of surface inclination (or the *slant*) but not the orientation of the inclination (or the *tilt*).

Suppose the surface is not a plane, i.e., parameters  $\alpha$ ,  $\beta$ ,  $\gamma$  are not zero at the same time. Still, there exist two exceptional cases (cf. Appendix C):

**Case 1.** If the surface has two principal curvatures of *equal magnitude*, parameters  $\tilde{\alpha}$ ,  $\tilde{\beta}$ ,  $\tilde{\gamma}$  are indeterminate (i.e., parameter  $\tau$  of eqn (6.8) becomes 0). In this case, we cannot tell whether the surface is *elliptic* (i.e., the Gaussian curvature is positive) or *hyperbolic* (i.e., the Gaussian curvature is negative).

**Case 2.** The four solutions for parameters  $\tilde{\alpha}$ ,  $\tilde{\beta}$ ,  $\tilde{\gamma}$  (two mirror image pairs) degenerate to two solutions (one mirror image pair) if and only if the surface is *parabolic*, i.e., the Hessian  $\alpha\gamma-\beta^2$  is zero (and hence the Gaussian curvature is also zero). In this case, the inner square root of eqn (6.8) becomes 0.

**Remark 6.1.** Parameters  $p$ ,  $q$  describe the gradient of the plane tangent to the surface at  $(0,0,r)$ . They are indeterminate only in the above two cases. In Case 1, parameters

$\tilde{\alpha}, \tilde{\beta}, \tilde{\gamma}$  are indeterminate, so that  $p, q$  are also indeterminate. In Case 2, parameters  $\tilde{\alpha}, \tilde{\beta}, \tilde{\gamma}$  are uniquely determined except for sign. However, the term  $\tilde{\alpha}\tilde{\gamma}-\tilde{\beta}^2$  in the denominators of eqns (6.9) become 0. Still, we can determine the ratio  $p:q$ , which indicates the *asymptotic direction* or the "ridge" of the surface. The fact that the gradient along the asymptotic direction is indeterminate is easily understood from the orthographic nature of the projection; the texture density is always constant along this orientation all over the image plane.

## 7. ALGORITHM OF CURVED SURFACE RECOVERY FROM TEXTURE

Now, we consider how to solve the basic equations (6.5) numerically.

### FIRST ORDER APPROXIMATION

If the window  $W$  is small and is located at the center of the image, the Taylor expansion in  $x, y$  yields

$$(\sqrt{1+A_1x+A_2y+A_3x^2+2A_4xy+A_5y^2})^\kappa = 1+Ax+By+Cx^2+Dxy+Ey^2+\dots, \quad (7.1)$$

where

$$\begin{aligned} A &= \frac{\kappa}{2}A_1, & B &= \frac{\kappa}{2}A_2, \\ C &= \frac{\kappa}{2}(A_3 + \frac{\kappa-2}{4}A_1^2), & D &= \kappa(A_4 + \frac{\kappa-2}{4}A_1A_2), & E &= \frac{\kappa}{2}(A_5 + \frac{\kappa-2}{4}A_2^2). \end{aligned} \quad (7.2)$$

If we put

$$\begin{aligned} L_i &= \int_W m_i(x, y) dx dy, & M_i &= \int_W x m_i(x, y) dx dy, & N_i &= \int_W y m_i(x, y) dx dy, \\ R_i &= \int_W x^2 m_i(x, y) dx dy, & S_i &= \int_W x y m_i(x, y) dx dy, & T_i &= \int_W y^2 m_i(x, y) dx dy \end{aligned} \quad (7.3)$$

for  $i=0,1,\dots,5$  and neglect higher order terms, the basic equations (6.5) become

$$\begin{bmatrix} M_1-(J_1/J_0)M_0 & N_1-(J_1/J_0)N_0 & R_1-(J_1/J_0)R_0 & S_1-(J_1/J_0)S_0 & T_1-(J_1/J_0)T_0 \\ M_2-(J_2/J_0)M_0 & N_2-(J_2/J_0)N_0 & R_2-(J_2/J_0)R_0 & S_2-(J_2/J_0)S_0 & T_2-(J_2/J_0)T_0 \\ M_3-(J_3/J_0)M_0 & N_3-(J_3/J_0)N_0 & R_3-(J_3/J_0)R_0 & S_3-(J_3/J_0)S_0 & T_3-(J_3/J_0)T_0 \\ M_4-(J_4/J_0)M_0 & N_4-(J_4/J_0)N_0 & R_4-(J_4/J_0)R_0 & S_4-(J_4/J_0)S_0 & T_4-(J_4/J_0)T_0 \\ M_5-(J_5/J_0)M_0 & N_5-(J_5/J_0)N_0 & R_5-(J_5/J_0)R_0 & S_5-(J_5/J_0)S_0 & T_5-(J_5/J_0)T_0 \end{bmatrix} \begin{bmatrix} A \\ B \\ C \\ D \\ E \end{bmatrix} = - \begin{bmatrix} L_1-(J_1/J_0)L_0 \\ L_2-(J_2/J_0)L_0 \\ L_3-(J_3/J_0)L_0 \\ L_4-(J_4/J_0)L_0 \\ L_5-(J_5/J_0)L_0 \end{bmatrix}. \quad (7.4)$$

Once  $A, B, C, D, E$  are obtained by solving eqns (7.4), the texture density parameters  $A_i, i=1,2,\dots,5$  are determined from eqns (7.2) by

$$\begin{aligned}
A_1 &= \frac{2}{\kappa} A, & A_2 &= \frac{2}{\kappa} B, \\
A_3 &= \frac{2}{\kappa} C - \frac{\kappa-2}{\kappa^2} A^2, & A_4 &= \frac{1}{\kappa} D - \frac{\kappa-2}{\kappa^2} AB, & A_5 &= \frac{2}{\kappa} E - \frac{\kappa-2}{\kappa^2} B^2.
\end{aligned} \tag{7.5}$$

#### ITERATIVE CORRECTION BY TAYLOR EXPANSION

The iterative correction scheme by Taylor expansion described in the last part of Section 5 can be applied to curved surfaces as well. Let  $\bar{A}_i$ ,  $i=1, \dots, 5$ , be the initial estimates for the texture density parameters. The Taylor expansion at these values yields

$$(\sqrt{1+A_1x+A_2y+A_3x^2+2A_4xy+A_5y^2})^\kappa = m_0(x,y) + \sum_{i=1}^5 m_i(x,y) \delta A_i + \dots \tag{7.6}$$

where  $\delta A_i = A_i - \bar{A}_i$ ,  $i=1, \dots, 5$ , and

$$\begin{aligned}
m_0(x,y) &= (\sqrt{1+\bar{A}_1x+\bar{A}_2y+\bar{A}_3x^2+2\bar{A}_4xy+\bar{A}_5y^2})^\kappa, \\
m_1(x,y) &= \frac{\kappa}{2} \frac{x}{(1+\bar{A}_1x+\bar{A}_2y+\bar{A}_3x^2+2\bar{A}_4xy+\bar{A}_5y^2)^{1-\kappa/2}}, \\
m_2(x,y) &= \frac{\kappa}{2} \frac{y}{(1+\bar{A}_1x+\bar{A}_2y+\bar{A}_3x^2+2\bar{A}_4xy+\bar{A}_5y^2)^{1-\kappa/2}}, \\
m_3(x,y) &= \frac{\kappa}{2} \frac{x^2}{(1+\bar{A}_1x+\bar{A}_2y+\bar{A}_3x^2+2\bar{A}_4xy+\bar{A}_5y^2)^{1-\kappa/2}}, \\
m_4(x,y) &= \frac{\kappa}{2} \frac{2xy}{(1+\bar{A}_1x+\bar{A}_2y+\bar{A}_3x^2+2\bar{A}_4xy+\bar{A}_5y^2)^{1-\kappa/2}}, \\
m_5(x,y) &= \frac{\kappa}{2} \frac{y^2}{(1+\bar{A}_1x+\bar{A}_2y+\bar{A}_3x^2+2\bar{A}_4xy+\bar{A}_5y^2)^{1-\kappa/2}}.
\end{aligned} \tag{7.7}$$

If we use as the test functions these  $m_i(x,y)$  themselves and put

$$J_i = \int_W f(x,y) m_i(x,y) dx dy, \quad i=0,1,\dots,5, \tag{7.8}$$

$$M_{ij} = \int_W m_i(x,y) m_j(x,y) dx dy, \quad i,j=0,1,\dots,5, \tag{7.9}$$

the basic equation (6.5) becomes

$$[A_{ij}][\delta A_i] = -[b_i], \tag{7.10}$$

where

$$A_{ij} = M_{ij} - (J_i/J_0)M_{0j}, \quad b_i = M_{i0} - (J_i/J_0)M_{00}. \tag{7.11}$$

If all  $\delta A_i$ ,  $i=1, \dots, 5$ , are sufficiently close to zero, the initial estimates are sufficiently accurate. Otherwise,  $A_i' = \bar{A}_i + \delta A_i$  are better approximations. As before, this process can be iterated by setting  $\bar{A}_i \leftarrow A_i'$  and repeating this procedure until convergence.

## 8. EXAMPLES OF COMPUTATION FOR SYNTHETIC IMAGES

Figs. 2 - 5 show texture images on a planar surface. We take the focal length  $f$  to be the unit of length. The window size is  $a=b=f \tan 10^\circ=0.176f$ . (The window is a rectangle of size  $2a \times 2b$ .) The camera axis is assumed to pass through the center of the square window. The true gradient is  $(p,q)=(1.500,0.866)$  for all the figures.

### REGULARLY ALIGNED DOT TEXTURE

Figs. 2a - 2c show projected images of regularly aligned dot textures on a planar surface. If we use  $m_0(x,y)=1$ ,  $m_1(x,y)=x$ ,  $m_2(x,y)=y$  as the test functions, i.e., if we compute the center of gravity of the texture, and iteratively correct these values by the method of camera rotation with  $m_0(x,y)=1$ ,  $m_1(x,y)=x-\sqrt{p}$ ,  $m_2(x,y)=y-\sqrt{q}$ , we successively obtain  $(p,q)$  as follows.

	Fig. 2a	Fig. 2b	Fig. 2c
1	(1.459, 1.088)	(1.610, 0.965)	(1.548, 0.958)
2	(1.402, 0.939)	(1.552, 0.875)	(1.499, 0.871)
3	(1.397, 0.937)	(1.548, 0.871)	(1.496, 0.867)
4	(1.397, 0.937)	(1.548, 0.871)	(1.496, 0.867)

If we apply the method of Taylor expansion to the same initial estimates with  $m_0(x,y)=L(x,y)$ ,  $m_1(x,y)=M(x,y)$ ,  $m_2(x,y)=N(x,y)$ , we obtain

	Fig. 2a	Fig. 2b	Fig. 2c
1	(1.459, 1.088)	(1.610, 0.965)	(1.548, 0.958)
2	(1.549, 0.767)	(1.549, 0.897)	(1.499, 0.869)
3	(1.527, 0.816)	(1.542, 0.887)	(1.496, 0.864)
4	(1.529, 0.807)	(1.541, 0.887)	(1.496, 0.864)

### RANDOM DOT TEXTURE

Figs. 3a - 3c show random dot textures on a planar surface. If we compute the center of gravity and use the method of camera rotation, the successive estimates of the gradient  $(p,q)$  become

	Fig. 3a	Fig. 3b	Fig. 3c
1	(1.558, 0.798)	(1.662, 0.945)	(1.535, 0.974)
2	(1.505, 0.695)	(1.617, 0.843)	(1.493, 0.891)
3	(1.504, 0.694)	(1.613, 0.840)	(1.491, 0.888)
4	(1.504, 0.694)	(1.613, 0.840)	(1.491, 0.888)

while the method of Taylor expansion yields

	Fig. 3a	Fig. 3b	Fig. 3c
1	(1.558, 0.798)	(1.662, 0.945)	(1.535, 0.974)
2	(1.422, 0.560)	(1.674, 0.832)	(1.527, 0.899)
3	(1.434, 0.583)	(1.667, 0.834)	(1.525, 0.897)
4	(1.430, 0.578)	(1.667, 0.834)	(1.525, 0.897)

## REGULARLY ALIGNED LINE SEGMENT TEXTURE

Figs. 4a - 4c show regularly aligned line segment textures on a planar surface. If we compute the center of gravity and use the method of camera rotation, the successive estimates of the gradient  $(p,q)$  become

Fig. 4a	Fig. 4b	Fig. 4c
1 (1.603, 0.994)	(1.762, 1.048)	(1.751, 1.045)
2 (1.379, 0.747)	(1.534, 0.899)	(1.527, 0.893)
3 (1.352, 0.756)	(1.505, 0.875)	(1.500, 0.869)
4 (1.351, 0.758)	(1.504, 0.874)	(1.499, 0.869)

while the method of Taylor expansion yields

Fig. 4a	Fig. 4b	Fig. 4c
1 (1.603, 0.994)	(1.762, 1.048)	(1.751, 1.045)
2 (1.569, 0.893)	(1.672, 0.960)	(1.666, 0.958)
3 (1.568, 0.893)	(1.669, 0.956)	(1.663, 0.954)
4 (1.568, 0.893)	(1.669, 0.956)	(1.663, 0.954)

## RANDOM LINE SEGMENT TEXTURE

Figs. 5a - 5c show random line segment textures on a planar surface. If we compute the center of gravity and use the method of camera rotation, the successive estimates of the gradient  $(p,q)$  become

Fig. 5a	Fig. 5b	Fig. 5c
1 (2.821, 0.602)	(2.196, 0.768)	(2.006, 0.910)
2 (2.275, 0.372)	(1.906, 0.590)	(1.710, 0.722)
3 (2.088, 0.271)	(1.856, 0.559)	(1.660, 0.684)
4 (2.111, 0.275)	(1.856, 0.559)	(1.661, 0.684)

while the method of Taylor expansion yields

Fig. 5a	Fig. 5b	Fig. 5c
1 (2.821, 0.602)	(2.196, 0.768)	(2.006, 0.910)
2 (2.477, 0.238)	(2.033, 0.561)	(1.825, 0.787)
3 (2.447, 0.257)	(2.022, 0.567)	(1.820, 0.781)
4 (2.445, 0.258)	(2.022, 0.567)	(1.820, 0.781)

## TEXTURE ON A CURVED SURFACE

Fig. 6 is an orthographic view of a regularly aligned dot texture on a quadric surface. Here, we take the window size  $a(=b)$  to be the unit of length. The true parameters are  $(\alpha a, \beta a, \gamma a) = (2, 0, 0)$ . (Note that parameters  $\alpha, \beta, \gamma$  have dimensions of  $1/\text{length}$ .) In this case, as discussed in Section 6, parameters  $p, q$  are indeterminate, but parameters  $\alpha, \beta, \gamma$  are uniquely determined except for sign. If we use the method of Section 7 with  $1, x, y, x^2, xy, y^2$  as the test functions for computation of the initial estimate and apply the method of Taylor expansion, the successive estimates of  $(\alpha a, \beta b, \gamma a)$  become

Fig. 6

- 1 (0.494, 0.000, -0.007)
- 2 (1.066, -0.000, -0.009)
- 3 (1.632, -0.001, -0.008)
- 4 (1.929, -0.001, -0.006)
- 5 (1.991, -0.001, -0.006)

## OBSERVATIONS

We see that our methods can produce fairly good results. In particular, our method can be applied to very sparsely distributed textures. For very sparse textures, the method of Taylor expansion gives more accurate results than the method of camera rotation. Otherwise, both of them yield almost the same results for dot textures, but for line segment textures the method of camera rotation predicts more accurate results than the method of Taylor expansion, as is expected (cf. Remark 5.2). The convergence is very rapid for both methods. Only two or three iterations are necessary to determine the gradient up to two decimal places, and three or four iterations up to three decimal places.

On the whole, the results are better for dot textures than for line segment textures. This is easily understood because a line segment is a coalescence of constituent points in a restricted way, so that the degree of homogeneity is lower for line segment textures than for dot textures in general. On the other hand, the results are far better for regular textures than random ones, as is also expected. This is not a drawback; natural or man-made textures we often encounter are usually "tessellated" to a high degree of regularity. The random texture shown here can be regarded, in a sense, as the "worst" case (cf. Remark 4.3).

## 9. COMPARISON WITH OTHER METHODS

Let us compare our method with those of Aloimonos and Swain [8] and Dunn [9]. Both proposed schemes of surface shape recovery from texture based on the geometry of perspective projection and the assumption of texture homogeneity. However, direct comparison is difficult because their derivations are based on different concepts and different assumptions. Therefore, we now newly derive, in our setting, those schemes which are essentially equivalent to (or actually better than) theirs.

### METHOD OF ALOIMONOS AND SWAIN

Consider three circular regions  $S_0, S_1, S_2$  on the image plane with centers  $(x_0, y_0), (x_1, y_1), (x_2, y_2)$ , respectively. Assume that they are sufficiently small compared with the size of the window  $W$ , yet the texture is sufficiently dense, so that each region contains a sufficiently large number of texture elements. Consider, as observables, the integrals

$$I_i = \int_{S_i} f(x, y) dx dy, \quad i=0, 1, 2. \quad (9.1)$$

Since each region  $S_i$  contains a large number of texture elements, these integrals can be approximated, according to eqn (4.8), by

$$I_i \approx c \int_{S_i} (\sqrt{\det(g)})^{\kappa} dx dy, \quad i=0, 1, 2. \quad (9.2)$$

This is equivalent to choosing as the test functions  $m_{\lambda}(x, y)$  the characteristic functions

$\chi_S(x, y)$  of regions  $S_i$  (cf. Remark 2.1). On the other hand, each region  $S_i$  is sufficiently small, so that the integral of eqn (9.2) can be replaced by the area  $S_i$  times the value at the center  $(x_i, y_i)$ , i.e.,

$$\int_{S_i} (\sqrt{\det(g)})^\kappa dx dy \approx S_i (\sqrt{\det(g)})^\kappa|_{x=x_i, y=y_i} \quad (9.3)$$

Thus, for a planar surface, the observables  $I_i$  are approximated by

$$I_i \approx c S_i \frac{(\sqrt{1+p^2+q^2})^\kappa (1+r/f)^{2\kappa}}{(1-(px_i+qy_i)/f)^{3\kappa}}, \quad i=0,1,2. \quad (9.4)$$

As a result, the basic equations (4.10) reduce to

$$\begin{aligned} \left( \left( \frac{I_1 S_0}{I_0 S_1} \right)^{\frac{1}{3\kappa}} x_1 - x_0 \right) p + \left( \left( \frac{I_1 S_0}{I_0 S_1} \right)^{\frac{1}{3\kappa}} y_1 - y_0 \right) q &= f \left( \left( \frac{I_1 S_0}{I_0 S_1} \right)^{\frac{1}{3\kappa}} - 1 \right), \\ \left( \left( \frac{I_2 S_0}{I_0 S_2} \right)^{\frac{1}{3\kappa}} x_2 - x_0 \right) p + \left( \left( \frac{I_2 S_0}{I_0 S_2} \right)^{\frac{1}{3\kappa}} y_2 - y_0 \right) q &= f \left( \left( \frac{I_2 S_0}{I_0 S_2} \right)^{\frac{1}{3\kappa}} - 1 \right), \end{aligned} \quad (9.5)$$

from which the gradient  $(p, q)$  is determined. This is essentially the method of Aloimonos and Swain [8]. They also tried recovery of curved surfaces, using a numerical relaxation scheme.

Thus, their method requires that the texture be *locally homogeneous* in the sense that the texture is sufficiently dense and the homogeneity condition is satisfied in any small region  $S$  (of an appropriate size). Furthermore, a very crude approximation like eqn. (9.3) is used. In our formulation, however, the texture need not be locally homogeneous. Some of the textures shown in the previous section are not locally homogeneous, so that application of the method of Aloimonos and Swain [8] is difficult. For our method, the homogeneity condition is required only over the entire window  $W$ , and the integration is exactly performed over all the texture elements in the window  $W$ .

#### METHOD OF DUNN

Dunn [9], on the other hand, considered a narrow strip  $S$  of width  $\delta$  and length  $l$  along line  $x \cos \theta + y \sin \theta = \rho$ . In our formulation, this process is regarded as integration of the texture density over the strip, i.e., integration of the characteristic function  $\chi_S(x, y)$  of the strip  $S$  as the test function  $m(x, y)$ . Take a new  $x'y'$ -coordinate system by rotating the  $xy$ -coordinate system counterclockwise by  $\theta$  (Fig. 7). Line  $x \cos \theta + y \sin \theta = \rho$  now becomes  $x' = \rho$  in the new coordinate system. Consider, as an observable, integration of the texture density over the strip  $S$  (i.e., integration of the characteristic function  $\chi_S(x, y)$  of the strip  $S$  as the test function  $m(x, y)$ ):

$$K(\rho, \theta) = \int_{-l/2}^{l/2} \int_{\rho-\delta/2}^{\rho+\delta/2} f(x, y) dx' dy'. \quad (9.6)$$

If there exist a sufficiently large number of texture elements in the strip  $S$ , the observable  $K(\rho, \theta)$  is approximated, according to eqn (4.8), by

$$K(\rho, \theta) \approx c \int_{-l/2}^{l/2} \int_{\rho-\delta/2}^{\rho+\delta/2} (\sqrt{\det(g)})^\kappa dx' dy'. \quad (9.7)$$

If the approximation (4.11) is used for a planar surface, this becomes

$$K(\rho, \theta) \approx c \delta l (\sqrt{1+p^2+q^2})^\kappa (1+r/f)^{2\kappa} (1+3\kappa(p \cos \theta + q \sin \theta) \rho / f). \quad (9.8)$$

As before, if  $K_i = K(\rho_i, \theta_i)$ ,  $i=0,1,2$ , are computed for three pairs of  $(\rho, \theta)$  (i.e., for the characteristic functions  $\chi_{S_i}(x, y)$  of the strips  $S_i$  as the test functions  $m_i(x, y)$ ), the basic equations (4.10) reduce to

$$\begin{aligned} (\rho_1 \cos \theta_1 - \frac{K_1}{K_0} \rho_0 \cos \theta_0) p + (\rho_1 \sin \theta_1 - \frac{K_1}{K_0} \rho_0 \sin \theta_0) q &= -\frac{f}{3\kappa} (1 - \frac{K_1}{K_0}), \\ (\rho_2 \cos \theta_2 - \frac{K_2}{K_0} \rho_0 \cos \theta_0) p + (\rho_2 \sin \theta_2 - \frac{K_2}{K_0} \rho_0 \sin \theta_0) q &= -\frac{f}{3\kappa} (1 - \frac{K_2}{K_0}), \end{aligned} \quad (9.9)$$

from which  $p, q$  are obtained.

Dunn [9], however, took another approach. He searched for  $\theta$  such that  $K(\rho, \theta)$  does not depend on  $\rho$ . If  $\theta_1$  is the one, we see from eqn (9.7) that  $\theta_1$  must satisfy

$$p \cos \theta_1 + q \sin \theta_1 = 0, \quad (9.10)$$

and hence

$$K(\rho, \theta_1) \approx c \delta l (\sqrt{1+p^2+q^2})^\kappa (1+r/f)^{2\kappa} (\equiv K_1) \quad (9.11)$$

is a constant. Next, search for  $\theta$  such that  $K(\rho, \theta)$  has the steepest ascent with respect to  $\rho$ . If  $\theta_2$  is the one, we see from eqn (9.7) that  $\theta_2 = \theta_1 \pm \pi/2$  and that

$$p \cos \theta_2 + q \sin \theta_2 = \sqrt{p^2+q^2}, \quad (9.12)$$

and hence

$$K(\rho, \theta_2) \approx K_1 (1+3\kappa \sqrt{p^2+q^2} \rho / f). \quad (9.13)$$

The orientation of the gradient  $(p, q)$  is given by eqn (9.9), and its magnitude is obtained by computing the (average) gradient of  $K(\rho, \theta_2)/K_1$ .

The latter method can be more robust to noise than the former one, for the former method depends only on three particular values of  $K(\rho, \theta)$  (i.e., three test functions), while in the latter method a large number of strips (i.e., many different test functions, cf. Remark 4.2) are used. Consequently, some sort of smoothing, say fitting to a parametric form, of  $K(\rho, \theta)$  can be used to cancel local errors in the process of searching for  $\theta_1$  and estimating the average gradient of  $K(\rho, \theta_2)/K_1$ . Dunn [9] also tried recovery of curved surfaces using a similar technique.

In any case, the underlying approximation is essentially the small gradient approximation. Although the integration is performed exactly up to linear approximation (i.e., eqn (9.8)), this method also requires that the texture be locally homogeneous (though mildly as compared with the method of Aloimonos and Swain [8]), so that the homogeneity condition must be satisfied in each strip.

## 10. CONCLUDING REMARKS

The methods proposed here have the following salient features.  
TEXTURE DENSITY AS A FUNCTIONAL

First, our formulation makes use of the *exact* texture density  $f(x,y)$  having singularities, and no smoothing is necessary. This is because we do not use particular *values* of the texture density itself; all we need is the *rule of integration*. Hence, the texture density is defined as a *functional*, or a *distribution* in the sense of Schwartz. This is one of the most important differences from all existing approaches. All early methods assume existence of a smooth texture density obtained by some kind of local averaging and directly use its values. Some approaches even require the values of the gradient of the texture density obtained by differentiation. The use of the values or derivatives of the texture density does not seem feasible in view of the discrete nature of the texture.

#### DIFFERENTIAL GEOMETRY IN TERMS OF IMAGE COORDINATES

We derived the exact relationship between the surface texture density and the observed texture density according to the principles of differential geometry. The existing methods seem to have failed to obtain this exact relationship. One reason, among others, seems to be that most authors employed a certain intrinsic "surface coordinate system" placed on the surface as well as an image coordinate system, trying to obtain the rule of transformation from the surface coordinates to the image coordinates. This usually results in tedious equations. The key to success here is the fact that we *do away with the surface coordinates*; all surface characteristics are described in terms of the image coordinates alone, the first fundamental form playing a fundamental role.

#### COMPUTATIONAL EFFICIENCY

Our method has also an advantage from the viewpoint of computational efficiency. The necessary data, or *observables*, are obtained by integration of functions over the image, and this is essentially summation of the function values over the texture elements. Thus, the time complexity is simply  $O(N)$ , where  $N$  is the number of texture elements. The access to each texture element is an independent process. This fact suggests high speed performance by "parallel architecture"; the image can be divided in any way and the computation can be performed independently and simultaneously. Although iterations are used in our method, the convergence is very rapid, as was demonstrated; two or three iterations seem sufficient.

#### PREPROCESSING

We should not forget the fact that appropriate preprocessing is necessary, as is also the case for any other high-level image processing. We regard texture as composed of dots *without area* and line segments *without width*. If the dots have area, their centroids can be used as their positions, or their boundaries can be regarded as texture elements. If the line segments have width, their center lines ("skeletons") or boundaries can be regarded as texture elements. This is because our method is essentially (weighted) *number counting* of dots and (weighted) *length measuring* of line segments. For "natural" texture images containing gray-levels, a simple way to do this preprocessing is to just apply edge detection. Then, the detected "edges" serve as line segment texture elements.

#### INTEGRATIONS AS OBSERVABLES

Another advantage resulting from the use of integrations as observables is that the method works for very *sparse* textures. All existing methods including those of Aloimonos and Swain [8] and Dunn [9] have paid attention to "local" clues such as the number or length of texture elements in small regions of the image. Hence, the texture must be *locally homogeneous*; the texture density must be dense enough everywhere so

that the homogeneity condition is satisfied in each of the observed regions. In our formulation, in contrast, the texture in its entirety is observed directly through integration over all the texture elements. Hence, the texture need not be dense everywhere, as was demonstrated in the previous examples, and the homogeneity condition need be satisfied only for the entire texture. (The idea of integrations as observables is also used by Kanatani [12] for "shape from motion without correspondence".) On the other hand, if we gradually increase the texture density, our estimation approaches the numerically *exact* value. No methods so far known seems to have this property. Those of Aloimonos and Swain [8] and Dunn [9] do not have this property, either, because various *ad hoc* approximations are involved.

#### DIMENSIONALITY OF TEXTURE ELEMENT

One of the important findings resulting from our analysis is the fact that dot textures and line segment textures cannot be treated in the same manner. Pixels constituting line segments on the image plane cannot be identified with pixels of a dot texture. The necessity of this distinction does not seem to have been widely recognized. All existing methods including those of Aloimonos and Swain [8] and Dunn [9] do not seem to take this effect correctly into account. It seems that the texture density, whether of dots or of line segments, has been treated in analogy with a continuous density. In this paper, we have established a rigorous treatment of discrete densities, making a clear distinction between dot textures and line segment textures. In fact, the recapitulation in Section 9 is actually a modification so that dimensionality of the texture elements is correctly incorporated.

#### GENERALITY OF THE PRINCIPLE

The main emphasis in this paper is the generality of our formulation, from which various modifications and applications become possible, including the choice of good test functions. The methods of Aloimonos and Swain [8] and Dunn [9], for example, can be regarded as special variants of our general principle. An important fact is that our formulation can also explain their methods and make explicit the underlying assumptions and approximations, while theirs can explain no other methods, only their own. This wide range of flexibility stems from a mathematically *correct* understanding of the geometry of perspective projection. Particular heuristics or *ad hoc* assumptions and approximations may result in particular algorithms which may be useful sometimes. Lacking generality, however, they usually do not reveal the underlying essential nature of the problem and are incapable of extension to other problems.

*Acknowledgement:* The authors express their thanks to Prof. Azriel Rosenfeld and Prof. Larry S. Davis of the University of Maryland for many comments. We also thank Prof. Thomas Seidman and Dr. Stanley Dunn of the University of Maryland and Dr. John Aloimonos of the University of Rochester for helpful discussions.

#### REFERENCES

1. A. P. Witkin, Recovering surface shape and orientation from texture, *Artificial Intelligence*, 17 (1981) 17 - 45.
2. L. S. Davis, L. Janos and S. M. Dunn, Efficient recovery of shape from texture, *IEEE Transactions on Pattern Analysis and Machine Intelligence*, PAMI-5 (1983) 485 - 492.

3. K. Kanatani, Detection of surface orientation and motion from texture by a stereological technique, *Artificial Intelligence*, **23** (1984) 213 - 237.
4. J. J. Gibson, *The Perception of the Visual World*, Houghton Mifflin, Boston, Mass., 1950.
5. J.J. Gibson, *The Senses Considered as Perceptual Systems*, Houghton Mifflin, Boston, Mass., 1966.
6. R. Bajcsy and L. Lieberman, Texture gradient as a depth cue, *Computer Graphics and Image Processing*, **5** (1976) 52 - 67.
7. K. A. Stevens, The information content of texture gradients, *Biological Cybernetics*, **42** (1981) 95 - 105.
8. J. Aloimonos and M. J. Swain, Shape from texture, *Proceedings of the Ninth International Joint Conference on Artificial Intelligence*, August 1985, Los Angeles, pp. 926 - 931.
9. S. M. Dunn, *Recovering the Orientation of Textured Surfaces*, Ph.D. thesis, Center for Automation Research, University of Maryland, 1985.
10. L. Schwartz, *Theorie des Distributions*, Vols. 1, 2, Hermann, Paris, 1950, 1951.
11. L. Schwartz, *Methodes Mathematiques pour les Sciences Physiques*, Hermann, Paris, 1961.
12. K. Kanatani, Structure from Motion without Correspondence: General Principle, *Proceedings of Image Understanding Workshop*, Miami Beach, FL, 1985, pp. 107 - 116.

## APPENDIX A. 3D GEOMETRY IN TERMS OF IMAGE COORDINATES

Here are some results from differential geometry which are relevant in the description of "shape from image", describing 3D properties in terms of the image coordinates.

### INNER PRODUCT, NORM, ANGLE

Consider two vectors  $U=(U_1, U_2, U_3)$ ,  $V=(V_1, V_2, V_3)$  tangent to the surface, making angle  $\theta$ . Suppose they are "small" in the sense that the first fundamental metric tensor  $g_{ij}$  is almost constant along them. Let  $(u^1, u^2)$ ,  $(v^1, v^2)$  be the projections of these vectors onto the image plane; they no longer make angle  $\theta$ . The inner product of  $U$  and  $V$  and their norms are computed from the projections onto the image plane as follows:

$$(U, V) = U_1 V_1 + U_2 V_2 + U_3 V_3 = \sum_{i,j=1}^2 g_{ij} u^i v^j \quad (A.1)$$

$$\|U\| = \sqrt{(U, U)}, \quad \|V\| = \sqrt{(V, V)}. \quad (A.2)$$

Hence, the angle  $\theta$  is computed from the projections of these vectors as

$$\cos\theta = (U, V) / (\|U\| \|V\|). \quad (A.3)$$

### LEVI-CIVITA PARALLELISM

Consider on the surface two nearby points whose projections onto the image plane are  $(x, y)$ ,  $(x+dx, y+dy)$ . Again, consider two vectors of the same length, "small" in the sense described above, tangent to the surface at these points. Let us hypothetically cut away from the surface a small patch which contains these two tangent vectors and the segment connecting them (to be precise, the *developable* defined as the *envelope* of the tangent planes along the segment). Then, *develop* that patch, i.e., "roll it out" on a plane (Fig. A). The two tangent vectors, having the same length, are now coplanar. If they are parallel, we say that one of the two tangent vectors is *transported* to the other along the segment *parallelly in the sense of Levi-Civita*. Let  $(u^1, u^2)$ ,  $(u^1 + \delta u^1, u^2 + \delta u^2)$  be the projections of these two tangent vectors. The condition that the corresponding

vectors undergo the parallel transport in the sense of Levi-Civita is given by

$$\delta u^i = - \sum_{j,k=1}^2 \left\{ \begin{matrix} i \\ j \ k \end{matrix} \right\} u^k dx^j, \quad (\text{A.4})$$

where  $\left\{ \begin{matrix} i \\ j \ k \end{matrix} \right\}$  is the *Christoffel symbol* defined by

$$\left\{ \begin{matrix} i \\ j \ k \end{matrix} \right\} = \frac{1}{2} \sum_{l=1}^2 g^{il} \left( \frac{\partial g_{jl}}{\partial x^k} + \frac{\partial g_{kl}}{\partial x^j} - \frac{\partial g_{jk}}{\partial x^l} \right), \quad (\text{A.5})$$

and  $g^{-1}=(g^{ij})$  is the inverse matrix of  $g=(g_{ij})$ . Assigning Levi-Civita parallelism by the Christoffel symbol as above is also said to define a *Riemann connection* on the image plane. This enables one to compute the curvature of the surface and the curvature of a curve on it in terms of the image coordinates (the *Gauss-Codazzi equations* and *Beltrami's formula*), but we do not go into details. (Refer to books on differential geometry.)

### GEODESICS

Consider a smooth curve on the surface, and let  $(x(s), y(s))$  be its projection onto the image plane, where the parameter  $s$  is taken to be the true arc length, defined by eqn (3.7), of the curve on the surface. Then,  $(\dot{x}(s), \dot{y}(s))$  is the projection of the unit length tangent vector to the curve. The curve is called a *geodesic* if its tangent vectors are always transported along the curve parallelly in the sense of Levi-Civita. Hence, it follows from eqn (A.4) that the projection of a geodesic is given by the following differential equation:

$$\ddot{x}^i(s) + \sum_{j,k=1}^2 \left\{ \begin{matrix} i \\ j \ k \end{matrix} \right\} \dot{x}^j(s) \dot{x}^k(s) = 0. \quad (\text{A.6})$$

It is known that a geodesic is the shortest path connecting the endpoints along the surface.

### GRADIENT

The orientation on the surface  $Z=Z(X, Y)$  along which the value of  $Z$  increases most rapidly on the surface is indicated by vector  $(P, Q, P^2+Q^2)/(1+P^2+Q^2)$ . The projection  $(u^1, u^2)$  of this vector onto the image plane is given by

$$u^i = \sum_{j=1}^2 g^{ij} \frac{\partial Z}{\partial x^j}. \quad (\text{A.7})$$

This vector indicates the orientation along which the surface "goes away" from the image plane.

## APPENDIX B. ERROR DUE TO RANDOMNESS OF THE TEXTURE

Consider a dot texture for simplicity. Let  $(x_1, y_1), \dots, (x_N, y_N)$  be the coordinates of the texture points in the window  $-a < x \leq a, -b < y \leq b$ . The center of gravity  $(\bar{x}, \bar{y})$  is given by

$$\bar{x} = \frac{1}{N} \sum_{i=1}^N x_i, \quad \bar{y} = \frac{1}{N} \sum_{i=1}^N y_i. \quad (\text{B.1})$$

First, consider the case where the distribution is completely random. Suppose  $x_i$ ,  $i=1, \dots, N$  are random variables chosen from the uniform distribution over  $-a < x \leq a$  independently from each other. Likewise, regard  $y_i$ ,  $i=1, \dots, N$  as random variables distributed uniformly and independently over  $-b < y \leq b$ . Then, their expectation values and variances are given by

$$\begin{aligned} E[x_i] &= 0, & V[x_i] &= \frac{1}{3}a^2, & i &= 1, \dots, N, \\ E[y_i] &= 0, & V[y_i] &= \frac{1}{3}b^2, & i &= 1, \dots, N. \end{aligned} \quad (\text{B.2})$$

It follows from elementary probability theory that the expectation values and the variances of  $\bar{x}$ ,  $\bar{y}$  are given by

$$\begin{aligned} E[\bar{x}] &= 0, & V[\bar{x}] &= \frac{1}{3N}a^2, \\ E[\bar{y}] &= 0, & V[\bar{y}] &= \frac{1}{3N}b^2. \end{aligned} \quad (\text{B.3})$$

Hence, the center of gravity is at the origin on the average. The magnitude of error is estimated by the *standard deviation*, so that we expect errors of about  $a/\sqrt{3N}$ ,  $b/\sqrt{3N}$  for  $\bar{x}$ ,  $\bar{y}$ , respectively.

On the other hand, consider another extreme case where  $x_i$ ,  $i=1, \dots, N$  are distributed with equal interval of distance  $2a/N$  and  $y_i$ ,  $i=1, \dots, N$  with equal interval of distance  $2b/N$ . Then, the center of gravity must be located within the range of

$$-\frac{a}{N} < \bar{x} \leq \frac{a}{N}, \quad -\frac{b}{N} < \bar{y} \leq \frac{b}{N}. \quad (\text{B.4})$$

From eqns (B.3) and (B.4), we can roughly say that the errors  $\delta\bar{x}$ ,  $\delta\bar{y}$  of  $\bar{x}$ ,  $\bar{y}$ , respectively, are

$$\delta\bar{x} = O\left(\frac{1}{N^\epsilon}\right), \quad \delta\bar{y} = O\left(\frac{1}{N^\epsilon}\right), \quad (\text{B.5})$$

where  $1/2 < \epsilon < 1$ . The parameter  $\epsilon$  approaches  $1/2$  as the distribution becomes more and more random, and it approaches  $1$  as the distribution becomes more and more regular.

## APPENDIX C. INTERPRETATION OF CURVED SURFACES

Define  $k$ ,  $\tilde{p}$ ,  $\tilde{q}$ ,  $\tilde{\alpha}$ ,  $\tilde{\beta}$ ,  $\tilde{\gamma}$  as follows:

$$k = \sqrt{1 + p^2 + q^2}, \quad (\text{C.1})$$

$$\tilde{p} = p/k, \quad \tilde{q} = q/k, \quad \tilde{\alpha} = \alpha/k, \quad \tilde{\beta} = \beta/k, \quad \tilde{\gamma} = \gamma/k.$$

Eqns (6.3) are now rewritten as follows:

$$\begin{aligned}\tilde{\alpha}\tilde{p}+\tilde{\beta}\tilde{q} &= \frac{A_1}{4}, & \tilde{\beta}\tilde{p}+\tilde{\gamma}\tilde{q} &= \frac{A_2}{4}, \\ \tilde{\alpha}^2+\tilde{\beta}^2 &= \frac{A_3}{4}, & \tilde{\beta}(\tilde{\alpha}+\tilde{\gamma}) &= \frac{A_4}{4}, & \tilde{\beta}^2+\tilde{\gamma}^2 &= \frac{A_5}{4},\end{aligned}\tag{C.2}$$

Let us define new variables

$$\tau = \frac{\tilde{\alpha}+\tilde{\gamma}}{2}, \quad \sigma = \frac{\tilde{\alpha}-\tilde{\gamma}}{2} + i\tilde{\beta},\tag{C.3}$$

where  $i$  is the imaginary unit, so that  $\sigma$  is a complex number. Next, put

$$T = \frac{A_3+A_5}{8}, \quad S = \frac{A_3-A_5}{8} + i\frac{A_4}{4},\tag{C.4}$$

so that  $S$  is also a complex number. Then, the last three equations of (C.2) are equivalent to

$$T = \tau^2 + \sigma\sigma^*, \quad S = 2\tau\sigma,\tag{C.5}$$

where  $*$  denotes the complex conjugate. From the second equation, we obtain  $\sigma = S/2\tau$ . Substituting this in the first equation, we find that  $\tau$  is the solution of

$$\tau^4 - T\tau^2 + \frac{1}{4}SS^* = 0.\tag{C.6}$$

and consequently

$$\tau^2 = \frac{1}{2}(T \pm \sqrt{T^2 - SS^*}),\tag{C.7}$$

or in terms of  $A_i$ ,  $i=1, \dots, 5$ ,

$$\tau^2 = \frac{1}{16}(A_3+A_5 \pm 2\sqrt{A_3A_5-A_4^2}).\tag{C.8}$$

Hence, eqn (6.8) is obtained, and  $\sigma$  is given by  $\sigma = S/2\tau$ . From eqns (C.3),  $\tilde{\alpha}$ ,  $\tilde{\beta}$ ,  $\tilde{\gamma}$  are given by

$$\tilde{\alpha} = \tau + \text{Re}[\sigma], \quad \tilde{\beta} = \text{Im}[\sigma], \quad \tilde{\gamma} = \tau - \text{Re}[\sigma],\tag{C.9}$$

from which eqns (6.7) are obtained.

Once  $\tilde{\alpha}$ ,  $\tilde{\beta}$ ,  $\tilde{\gamma}$  are obtained,  $\tilde{p}$ ,  $\tilde{q}$  are determined from the first two equations of (C.2) in the form of eqns (6.9). Finally, noting

$$1 - \tilde{p}^2 - \tilde{q}^2 = 1 - \frac{p^2}{1+p^2+q^2} - \frac{q^2}{1+p^2+q^2} = \frac{1}{1+p^2+q^2} = \frac{1}{k^2},\tag{C.10}$$

we obtain eqn (6.10). Thus,  $p$ ,  $q$ ,  $\alpha$ ,  $\beta$ ,  $\gamma$  are given by eqns (6.6).

#### APPENDIX D. AMBIGUITY OF CURVED SURFACE RECOVERY

Consider the pathological cases ignored in Appendix C. First,  $\tau$  was assumed not to be zero, since otherwise  $\sigma = S/2\tau$  is indeterminate. From eqn (C.7),  $\tau$  becomes zero if and only if  $S=0$  or

$$A_3 = A_5, \quad A_4 = 0.\tag{D.1}$$

In this case, eqns (C.2) reduce to

$$\tilde{\alpha}^2 + \tilde{\beta}^2 = \tilde{\beta}^2 + \tilde{\gamma}^2 = T, \quad \tilde{\beta}(\tilde{\alpha} + \tilde{\gamma}) = 0. \quad (\text{D.2})$$

If  $T=0$ , then  $\tilde{\alpha}=\tilde{\beta}=\tilde{\gamma}=0$  and hence the surface is planar. Suppose  $T \neq 0$ . If  $\tilde{\beta}=0$ , then  $\tilde{\alpha}=\pm\sqrt{T}$  and  $\tilde{\gamma}=\pm\sqrt{T}$ . If  $\tilde{\beta} \neq 0$ , then  $\tilde{\alpha}+\tilde{\gamma}=0$  and  $\tilde{\alpha}^2+\tilde{\beta}^2=T$ . These two cases correspond to surfaces whose two principal curvatures have the same magnitude. In other words, ambiguity of  $\tilde{\alpha}$ ,  $\tilde{\beta}$ ,  $\tilde{\gamma}$  occurs for a non-planar surface if and only if the surface has principal curvatures of the same magnitude, in which case we cannot tell whether the surface is *elliptic* (i.e., the Gaussian curvature is positive) or *hyperbolic* (i.e., the Gaussian curvature is negative).

Next, suppose we have determined  $\tilde{\alpha}$ ,  $\tilde{\beta}$ ,  $\tilde{\gamma}$ . When solving the first two equations of (C.2) for  $p$ ,  $q$ , we assumed  $\tilde{\alpha}\tilde{\gamma}-\tilde{\beta}^2 \neq 0$ . The condition that  $\tilde{\alpha}\tilde{\gamma}-\tilde{\beta}^2=0$ , or equivalently  $\alpha\gamma-\beta^2=0$ , means that the *Hessian* of the surface is zero (and hence the Gaussian curvature is also zero). This occurs for a non-planar surface if and only if one of the principal curvatures is zero and hence the surface is parabolic. For the parabolic case, only the ratio  $p:q$  is determined, indicating the *asymptotic direction* of the surface. In this case, the proportionality constant  $k$  is indeterminate, so that  $\alpha$ ,  $\beta$ ,  $\gamma$  are also indeterminate. (However, if  $p$  and  $q$  are known to be small, we may use the approximation of  $k \approx 1$  and hence  $\alpha \approx \tilde{\alpha}$ ,  $\beta \approx \tilde{\beta}$ ,  $\gamma \approx \tilde{\gamma}$ .)

Eqn (6.8) indicates existence of four solutions. They consist of two pairs of mutual mirror images with respect to a plane perpendicular to the  $z$ -axis. The remaining ambiguity is due to the fact that the texture density only tells about the absolute value of the *slant* and that no information is obtained about the *tilt*. From eqn (C.7), this ambiguity does not occur if and only if  $T^2=SS^*$ . In view of eqns (C.5), this is equivalent to  $r^2=\sigma\sigma^*$ . From eqns (C.3), this is equivalent in turn to  $\tilde{\alpha}\tilde{\gamma}-\tilde{\beta}^2=0$ . In other words, the ambiguity does not occur for a non-planar surface, except for the mirror image, if and only if the surface is parabolic.

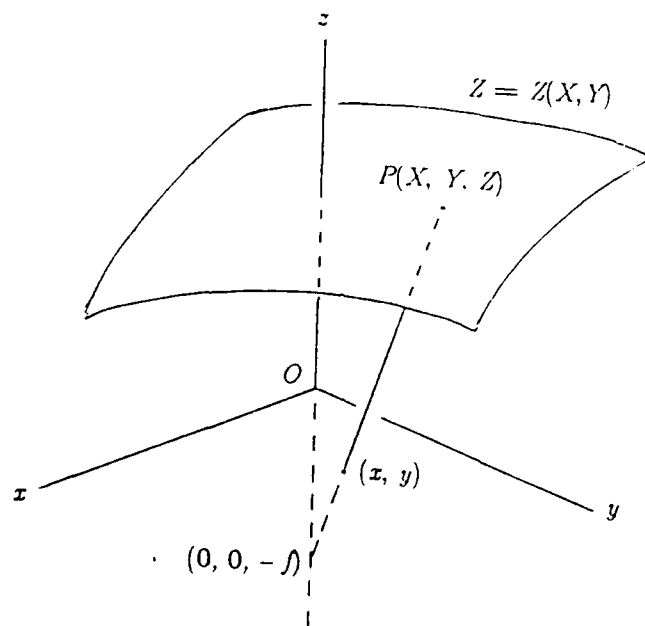
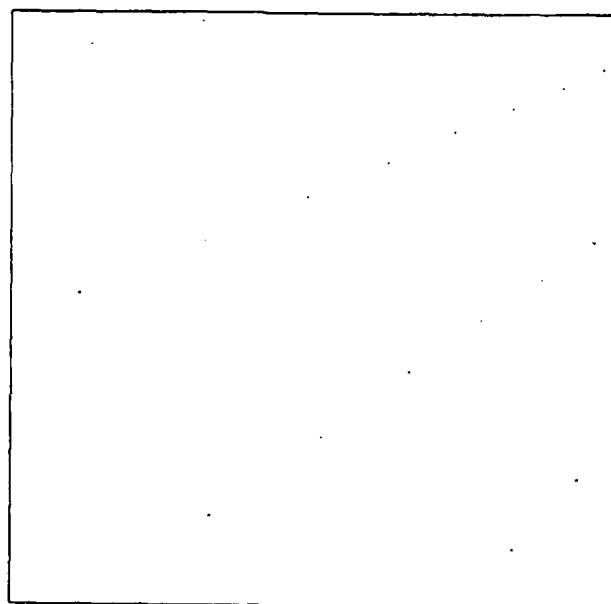
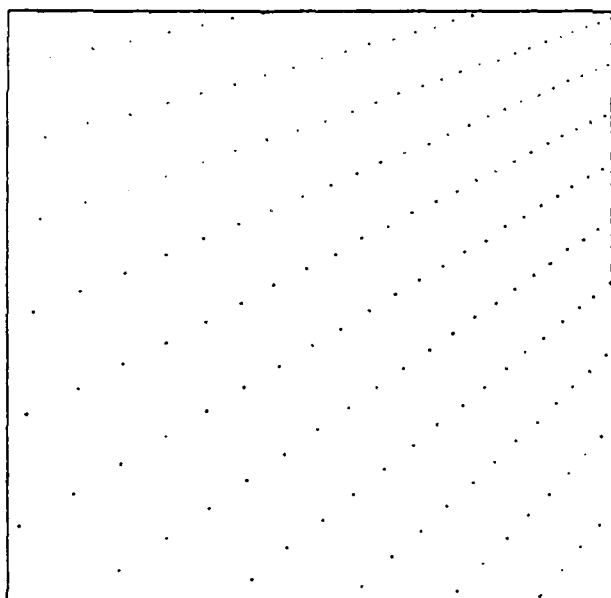


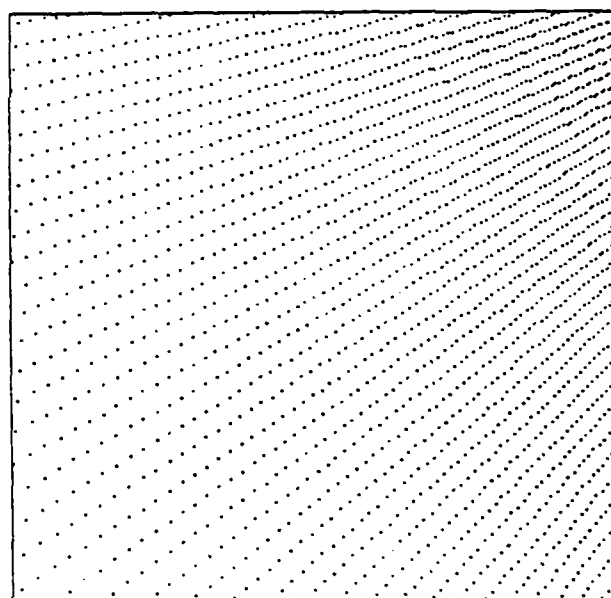
Fig. 1 Point  $(X, Y, Z)$  on the surface  $Z = Z(X, Y)$  is projected onto point  $(x, y)$  on the  $xy$ -plane by perspective projection, point  $(0, 0, -f)$  being the viewpoint.



(a)

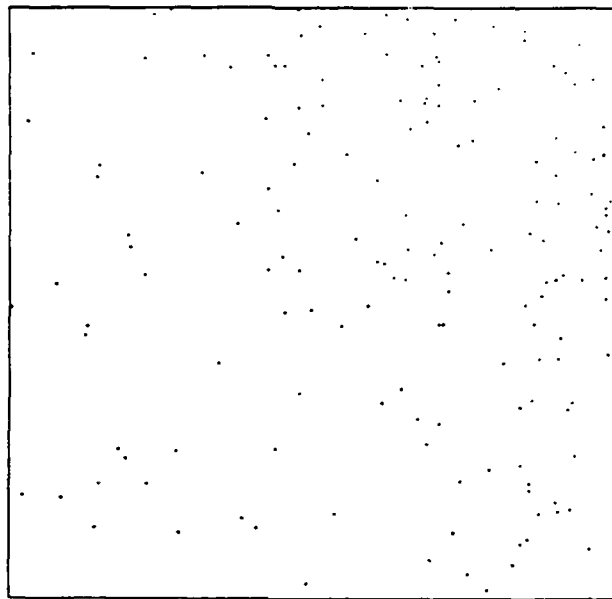


(b)

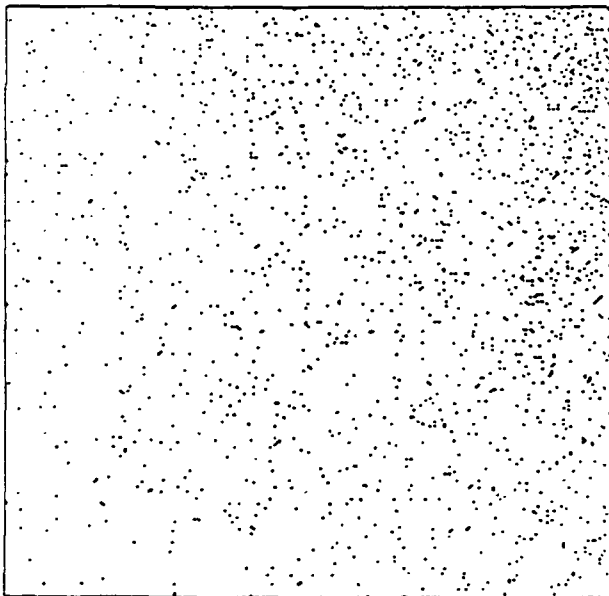


(c)

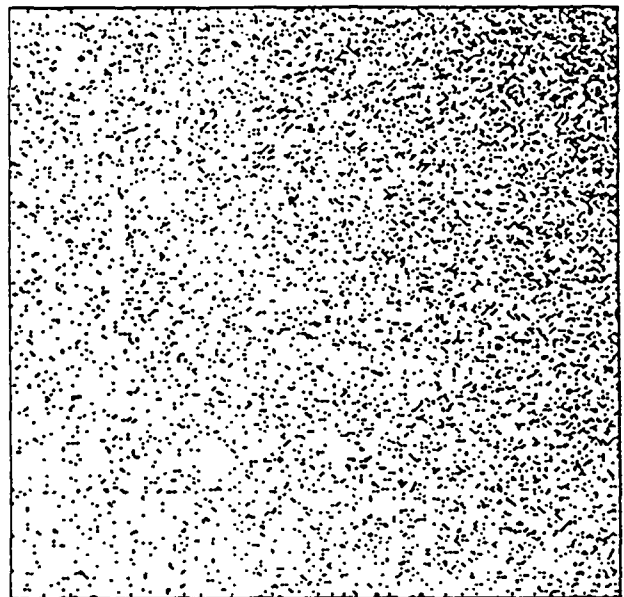
Fig. 2 Regularly aligned dot textures on a planar surface.



(a)

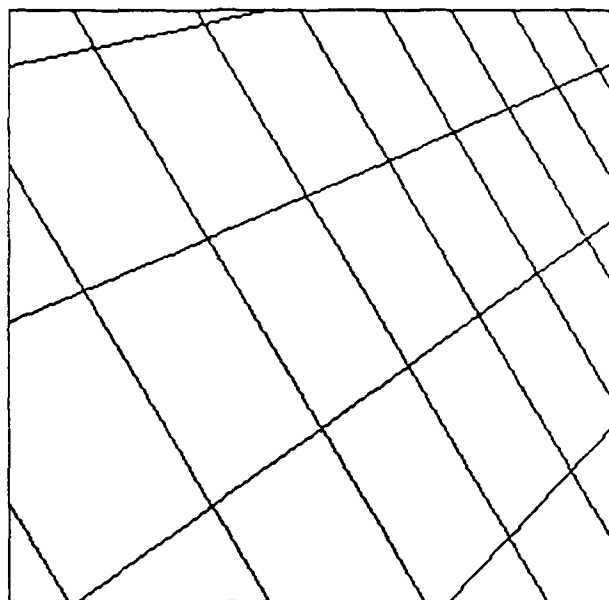


(b)

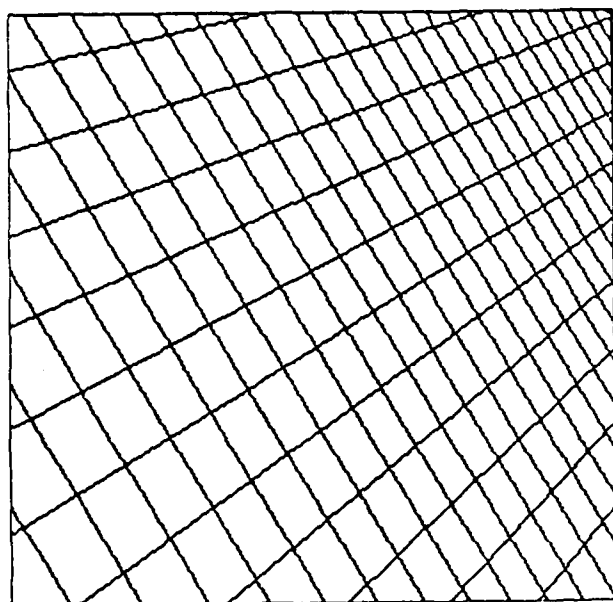


(c)

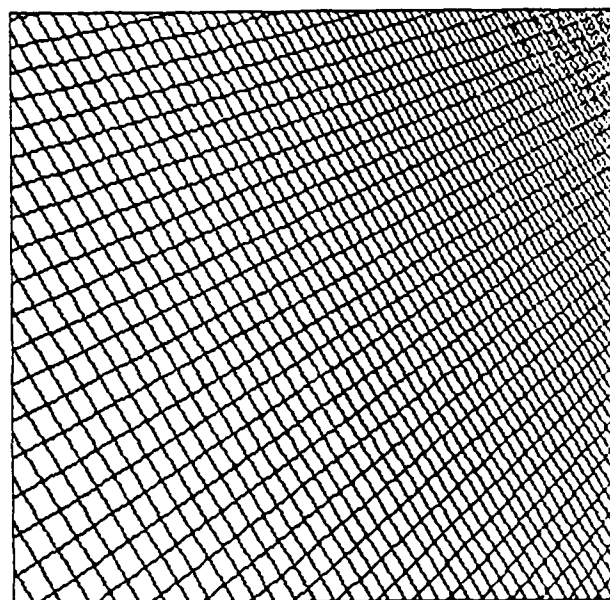
Fig. 3 Random dot textures on a planar surface.



(a)

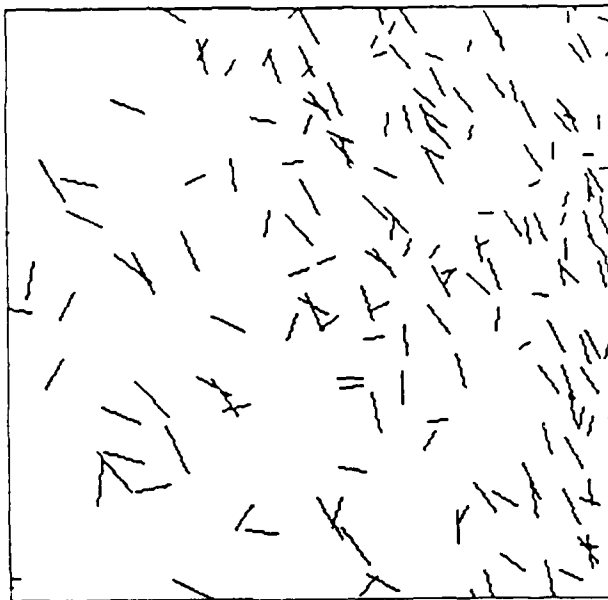


(b)

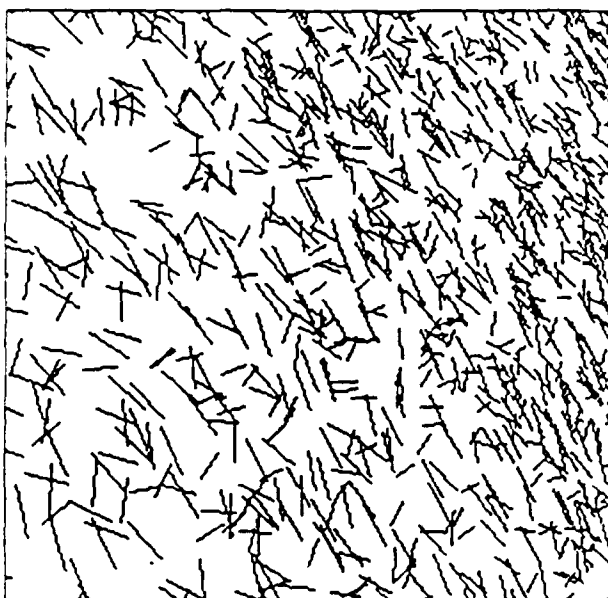


(c)

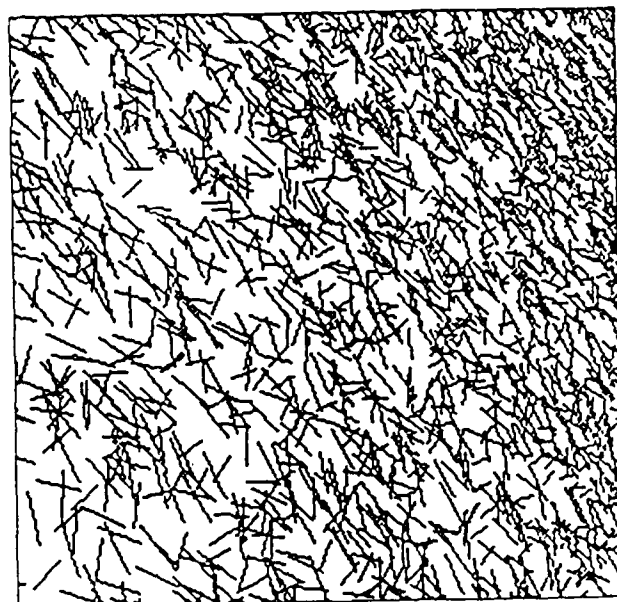
Fig. 4 Regularly aligned line textures on a planar surface.



(a)



(b)



(c)

Fig. 5 Random line segment textures on a planar surface.

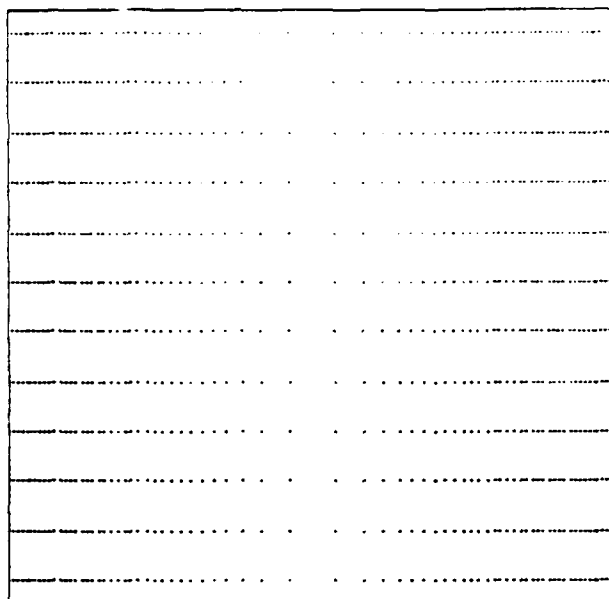


Fig. 6 An orthographic view of a regularly aligned dot texture on a curved surface.

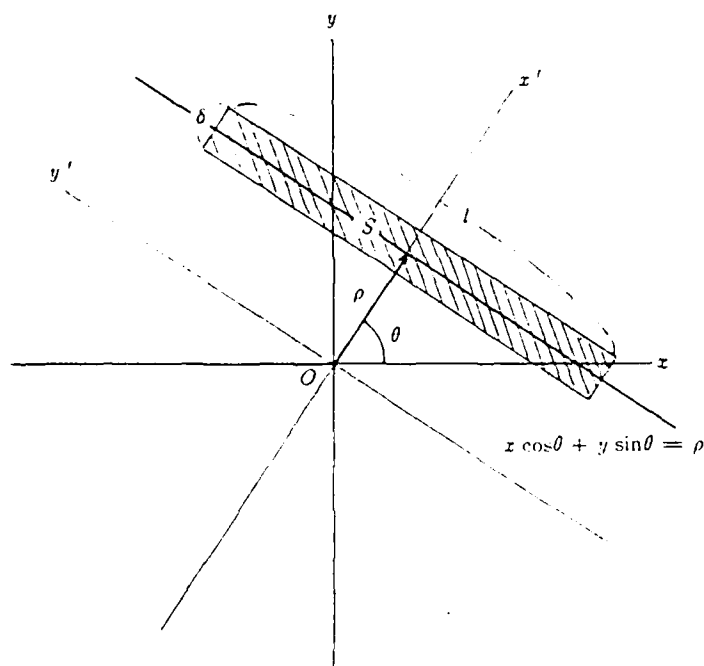


Fig. 7 A strip  $S$  of width  $\delta$  and length  $l$  around  $x \cos \theta + y \sin \theta = \rho$ .

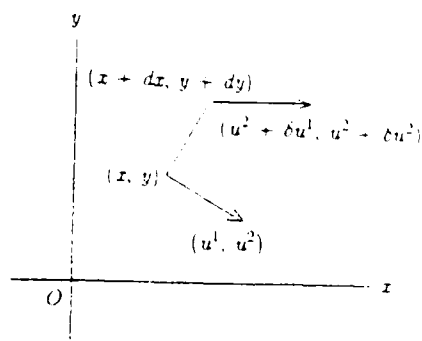


Fig. A Two small vectors infinitesimally far apart and tangent to the surface are *parallel in the sense of Levi-Civita* if they are parallel and of the same length after the small patch containing them is *developed*, i.e., "cut out" and "rolled out" on a plane.

UNCLASSIFIED

SECURITY CLASSIFICATION OF THIS PAGE

DD FORM 1473 83 APR

## REPORT DOCUMENTATION PAGE

1a. REPORT SECURITY CLASSIFICATION UNCLASSIFIED		1b. RESTRICTIVE MARKINGS N/A													
2a. SECURITY CLASSIFICATION AUTHORITY N/A		3. DISTRIBUTION/AVAILABILITY OF REPORT Approved for public release; distribution unlimited													
2b. DECLASSIFICATION/DOWNGRADING SCHEDULE N/A															
4. PERFORMING ORGANIZATION REPORT NUMBER(S) CAR-TR-184 CS-TR-1618		5. MONITORING ORGANIZATION REPORT NUMBER(S) N/A													
6a. NAME OF PERFORMING ORGANIZATION University of Maryland	6b. OFFICE SYMBOL (If applicable) N/A	7a. NAME OF MONITORING ORGANIZATION Army Night Vision and Electro-Optics Laboratory													
6c. ADDRESS (City, State and ZIP Code) Center for Automation Research College Park, MD 20742		7b. ADDRESS (City, State and ZIP Code) Fort Belvoir, VA 22060													
8a. NAME OF FUNDING SPONSORING ORGANIZATION Defense Advanced Research Projects Agency	8b. OFFICE SYMBOL (If applicable) IPTO	9. PROCUREMENT INSTRUMENT IDENTIFICATION NUMBER DAAK70-83-K-0018													
8c. ADDRESS (City, State and ZIP Code) 1400 Wilson Blvd. Arlington, VA 22209		10. SOURCE OF FUNDING NOS. <table border="1"><tr><td>PROGRAM ELEMENT NO</td><td>PROJECT NO</td><td>TASK NO</td><td>WORK UNIT NO</td></tr><tr><td></td><td></td><td></td><td></td></tr></table>		PROGRAM ELEMENT NO	PROJECT NO	TASK NO	WORK UNIT NO								
PROGRAM ELEMENT NO	PROJECT NO	TASK NO	WORK UNIT NO												
11. TITLE (Include Security Classification) Shape from Texture: General Principle															
12. PERSONAL AUTHOR(S) Ken-ichi Kanatani and Tsai-Chia Chou															
13a. TYPE OF REPORT Technical	13b. TIME COVERED FROM _____ TO N/A	14. DATE OF REPORT (Yr., Mo., Day) February 1986	15. PAGE COUNT 39												
16. SUPPLEMENTARY NOTES															
17. COSATI CODES <table border="1"><tr><th>FIELD</th><th>GROUP</th><th>SUB. GR.</th></tr><tr><td></td><td></td><td></td></tr><tr><td></td><td></td><td></td></tr><tr><td></td><td></td><td></td></tr></table>		FIELD	GROUP	SUB. GR.										18. SUBJECT TERMS (Continue on reverse if necessary and identify by block number)	
FIELD	GROUP	SUB. GR.													
19. ABSTRACT (Continue on reverse if necessary and identify by block number) The 3D shape of a textured surface is recovered from its projected image on the assumption that the texture is homogeneously distributed. First, the homogeneity of a discrete texture consisting of dots and line segments is defined in terms of the theory of distributions. Next, distortion of the observed texture density due to perspective projection is described in terms of the first fundamental form, which is expressed with respect to the image coordinate system. Based on this result, the basic equations to determine the surface shape are derived for both planar and curved surfaces, and numerical schemes are proposed to solve them. Necessary data are obtained in the form of summation or integration of functions over the texture elements on the image plane. Ambiguity in the interpretation of curved surfaces is also analyzed. Finally, numerical examples for synthetic data are presented, and our method is compared with other existing methods. It is shown that all other methods can be explained in terms of our formulation.															
20. DISTRIBUTION/AVAILABILITY OF ABSTRACT UNCLASSIFIED/UNLIMITED <input checked="" type="checkbox"/> SAME AS RPT. <input type="checkbox"/> DTIC USERS <input type="checkbox"/>		21. ABSTRACT SECURITY CLASSIFICATION UNCLASSIFIED													
22a. NAME OF RESPONSIBLE INDIVIDUAL		22b. TELEPHONE NUMBER (Include Area Code)	22c. OFFICE SYMBOL												

DD FORM 1473, 83 APR

EDITION OF 1 JAN 73 IS OBSOLETE.

UNCLASSIFIED  
SECURITY CLASSIFICATION OF THIS PAGE

END

DTIC

10-86